



Sixth framework programme of the  
European Commission

GOCE-CT-2003-505401

## RIVERTWIN

### **A regional model for integrated water management in twinned river basins**

**Instrument:** Specific Targeted Research Project (STREP)

**Priority:** Sustainable development, Global Change and Ecosystems

#### **D30 Highly resolved climate scenarios from stochastic model Until 2030 for the Chirchik river basin**

Due date of deliverable: Feb 06

Actual submission date: July 06

Start date of project: 01.03.2004

Duration: 3 years

***Institute of Hydraulic Engineering, University of Stuttgart***

**Revision: Final**

| <b>Project co-funded by the European Commission within the Sixth Framework programme (2002-2006)</b> |  |          |
|--|--|----------|
| Dissemination level  |  |          |
| PU   | Public   | <b>X</b> |
| PP   | Restricted to other programme participants (including Commission Services)       |          |
| RE   | Restricted to group specified by the consortium (including Commission Services)  |          |
| CO   | Confidential, only for members of the consortium (including Commission Services) |          |

# Table of content

|          |  |           |
|----------|--|-----------|
| <b>1</b> | <b>INTRODUCTION .....</b>  | <b>3</b>  |
| <b>2</b> | <b>DATA SETS AND STUDY AREA .....</b>                            | <b>3</b>  |
| 2.1      | CLIMATE CONDITION .....  | 3         |
| 2.2      | DATA AVAILABILITY .....  | 5         |
| <b>3</b> | <b>METHODOLOGY .....</b>   | <b>7</b>  |
| 3.1      | CIRCULATION PATTERNS.....  | 7         |
| 3.1.1    | Classification of circulation patterns .....                     | 7         |
| 3.1.2    | Grouping of circulation patterns.....                            | 7         |
| 3.2      | STATISTICAL DOWNSCALING MODEL .....                              | 7         |
| <b>4</b> | <b>RESULT .....</b>  | <b>11</b> |
| 4.1      | PRECIPITATION DOWNSCALING MODEL .....                            | 11        |
| 4.1.1    | Performance of classified circulation patterns .....             | 11        |
| 4.1.2    | Impact of moisture flux derived from large-scale parameters..... | 13        |
| 4.1.3    | Calibration and validation of model's performance .....          | 14        |
| 4.1.4    | Climate scenarios .....  | 18        |
| 4.2      | TEMPERATURE DOWNSCALING MODEL.....                               | 22        |
| 4.2.1    | Performance of classified circulation patterns .....             | 22        |
| 4.2.2    | Validation of model's performance .....                          | 22        |
| 4.2.3    | Climate scenarios .....  | 24        |
| <b>5</b> | <b>CONCLUSION.....</b>   | <b>27</b> |
|          | <b>APPENDIX I:.....</b>  | <b>28</b> |
|          | <b>APPENDIX II:.....</b>   | <b>30</b> |

## 1 Introduction

The aim of this paper is to report on the application of climate downscaling in the Chirchik-Ahangaran Basin in Central Asia in order to acquire meteorological variables with high resolution at both spatial and temporal scales. The methodology has been developed and further applied in the Neckar river Basin in Germany and testified a promising performance under the condition with good data availability. The same methodology will now be used for the Chirchik-Ahangaran basin in order to study the feasibility of transferring this model concept to another river basin with completely different climate characteristics and data availability.

## 2 Data sets and study area

### 2.1 Climate conditions

The Chirchik – Ahangaran basin is located in the north-eastern part of the Republic of Uzbekistan in Central Asia, between the Syrdarya River and the western Tien Shan Mountains. See **Fig. 1**. The whole river basin stretches out within the area of three republics, Kazakhstan, Kyrgyzstan, and Uzbekistan, but is mainly located in the regime of the Republic of Uzbekistan.

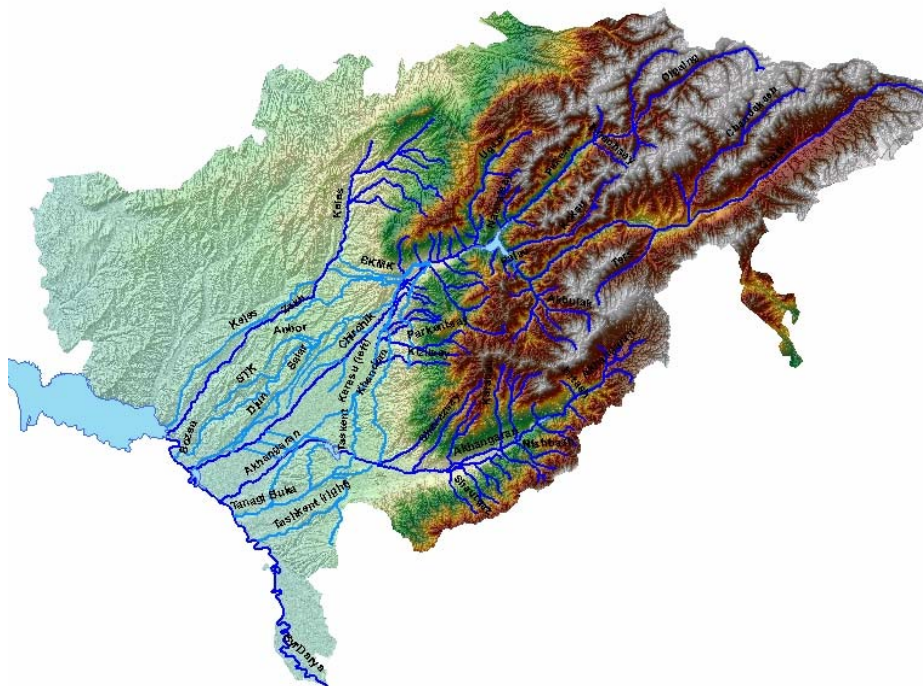


**Figure 1: Overview of Chirchik-Ahangaran regions in the Republic of Uzbekistan (Tuchin, ICWC SC)**

The river basin can be considered in two parts based on its geographical conditions: the upper Chirchik and the lower Chirchik. The upper part is located in the north-eastern mountainous area, the lower part in the south-western part, characterised by flat plains.

The climate conditions in Chirchik are of a continental, sub-tropical type that is impacted by the cyclone and anticyclones formed above continents at higher latitude regions. Five exemplary stations are chosen to demonstrate meteorological condition over a year, for instance, precipitation and average temperature. These 5 stations are Oygaing, Pskem, Tashkent, Dukant and Angren. Oygaing and Pskem are located in north-eastern mountainous areas and others are in the south-western plain area.

In general, the peak rainfall is falling in early spring, while the lower rainfall amounts occur during the summer months and under extreme cases, even can be reduced to zero. **[Fig. 2]** In addition, the local precipitation is distributed unevenly in the spatial resolution. More precipitation occurs in the northern and western parts of region due to a westerly wind carrying a more moisture flux.

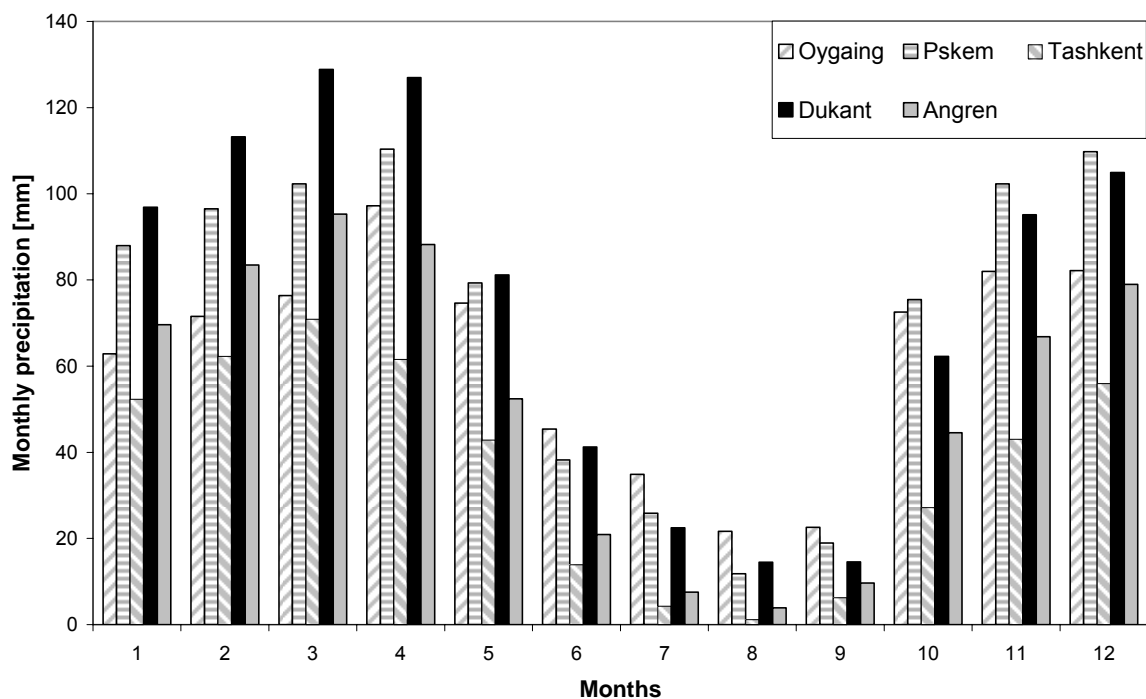


**Figure 2: Annual cycle of monthly rainfall observed at stations Oygaing, Pskem, Tashkent, Dukant and Angren, distributed from North to South**

Like most regions in subtropical climate zones in the northern hemisphere, there are distinct seasonal changes in temperature in the Chirchik-Ahangaran basin. **[Fig. 3]**

The summer is the hottest season of the whole year, especially on the plain, with temperatures normally hotter than those in the mountainous areas. On the plain, the average temperature is more than 25 °C and the maximum temperature can even reach 40 °C. Similarly, the areas on the plain are warmer than those in the mountains during the winter months. The average temperature can be down to -10 °C in the mountains compared with 2 °C on the plain.

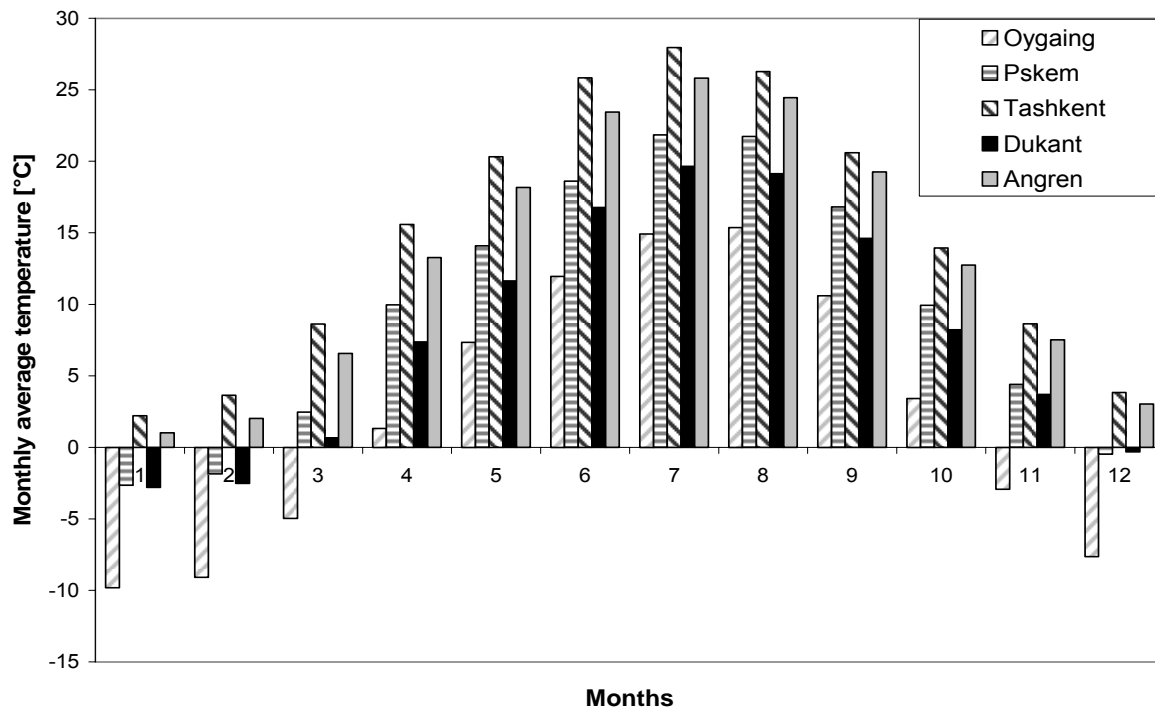


**Figure 3: Annual cycle of monthly average temperature observed at stations Oygaiing, Pskem, Tashkent, Dukant and Angren, distributed from North to South**

## 2.2 Data availability

Data sources used for the downscaling process contain two main categories: local measured meteorological parameters, e.g., daily precipitation and daily temperature; and large-scale meteorological parameters like mean sea level pressure (MSLP), geopotential height (GPH), geopotential wind field (U,V) and specific humidity (SH).

There are several ground-based meteorological stations located within the study area, however, only a few of them at daily scale are accessible for us. Most of the metrological stations have records from the 1950s up to the year 1991 and resume from the year 2000 to present. However, there are many missing values in the records.

Generally speaking, the quality of data is not very good. The time slices and data sources are listed in the following tables. See **Tab.1 – 3**.

All the results and their quality reported in this paper are constrained by the limited availability of data resources.

The large-scale meteorological parameters are derived from NCEP re-analysis archives, provided by National Centers for Environmental Prediction in the United States. MSLP serves as predictor for the classification of precipitation circulation patterns, and geopotential height at 700 hPa as a predictor for the classification of temperature circulation patterns. In addition, the product of geotropic wind and specific humidity is applied as a potential predictor to enhance the model's performance.

**Table 1: Meteorological data provided by Hydromet in Uzbekistan (1980-2003)**

| Station_ID | Precipitation | Tmax_Min | Pressure | Humidity | Wind | Temperal resolution |
|------------|---------------|----------|----------|----------|------|---------------------|
| Angren     | +             | +        | +        | +        | +    | Monthly (1980-2003) |
| Dukant     | +             | +        | +        | +        | +    | Monthly (1980-2003) |
| Oygaing    | +             | +        | +        | +        | +    | Monthly (1980-2003) |
| Pskem      | +             | +        | +        | +        | +    | Monthly (1980-2003) |
| Tashkent   | +             | +        | +        | +        | +    | Monthly (1980-2003) |

**Table 2: Meteorological data obtained from Russian's weather server**

| Station_ID | Precipitation | Tmax_Min | Temperal resolution |
|------------|---------------|----------|---------------------|
| Angren     | +             | +        | Daily (2000-2004)   |
| Dukant     | +             | +        | Daily (2000-2004)   |
| Oygaing    | +             | +        | Daily (2000-2004)   |
| Pskem      | +             | +        | Daily (2000-2004)   |
| Tashkent   | +             | +        | Daily (2000-2004)   |
| Bekabad    | +             | +        | Daily (2000-2004)   |
| Chimgan    | +             | +        | Daily (2000-2004)   |
| Kamchik    | +             | +        | Daily (2000-2004)   |

**Table 3: Meteorological data obtained from Global Daily Climatology Network (KNMI)**

| Station_ID            | Precipitation | Tmax_Min | Completeness | Temperal resolution |
|-----------------------|---------------|----------|--------------|---------------------|
| Tashkent              | +             | +        | good         | Daily (1891-1991)   |
| Dukant                | +             | -        | poor         | Daily (1959-1991)   |
| Oygaing               | +             | -        | poor         | Daily (1962-1991)   |
| Pskem                 | +             | -        | fair         | Daily (1936-1991)   |
| Kamchik               | +             | -        | poor         | Daily (2000-2004)   |
| Kizil'cha             | +             | -        | poor         | Daily (1958-1991)   |
| Ust'E_P.ters          | +             | -        | poor         | Daily (1936-1991)   |
| Charvak               | +             | -        | fair         | Daily (1936-1991)   |
| Kauncy                | +             | -        | poor         | Daily (1959-1991)   |
| Paca-ata (Kyrgyzstan) | +             | -        | fair         | Daily (1914-1991)   |
| Urtatoky (Kyrgyzstan) | +             | -        | fair         | Daily (1959-1987)   |

### 3 Methodology

#### 3.1 Circulation patterns

##### 3.1.1 Classification of circulation patterns

Fuzzy - rule based classification, one of the objective classifications, is adopted to generate representative circulation patterns (CP). It works on the concept of fuzzy sets (Zadeh, 1965), using imprecise statements to describe the climate system. The classification scheme for circulation patterns (CPs) follows 4 steps: the transformation of large-scale data, the definition of fuzzy rules, and the optimization of fuzzy rules and classification of circulation patterns.

Within the fuzzy-rule based classification scheme, anomalies of normalized meteorological variables like sea level pressure (MSLP) and geopotential height (GPH) serve as predictors for precipitation and temperature classification respectively. Each CP is described with a fuzzy rule.

To determine the best possible rule sets, the defined CPs must be optimized with local variables. These local variables can be daily precipitation, daily discharge or daily temperature, which are supposed to represent the behavior of regional meteorological variables of interest.

##### 3.1.2 Grouping of circulation patterns

Under some conditions, the classified circulation patterns seldom occur over the study area; this makes it difficult to obtain enough original data and to further identify the reliable statistical relationship for single CP. Therefore, original circulation patterns need to be regrouped to fewer types.

#### 3.2 Statistical downscaling model

The statistical downscaling process is set up based on a conditional probabilistic concept and several steps are required in order to attain a reliable output:

- Classifying atmospheric circulation patterns (CPs)
- Coupling the conditional model with additional large-scale variables
- Calibrating model parameters for specific statistic distribution
- Downscaling meteorological parameters derived from climate scenarios A2 and B2 generated by the Global Circulation Model, ECHAM4 to study future climate conditions

The **rainfall** generating model is a stochastic model that links local rainfall events with classified atmospheric CPs using conditional distribution and conditional spatial covariance functions. It is a transformed conditional multivariate autoregressive model with CP-dependent parameters.

The precipitation is distinctly asymmetrical, skewed to the right and physically constrained to be non-negative. That is, small daily rainfall amounts quite often occur, while the larger daily

rainfall amount that are most important to flooding and hydraulics are more seldom. In order to capture the specific behavior of precipitation, many precipitation generators have been developed, such as exponential distribution (Todorovic and Woolhiser, 1975), gamma distribution (Tatz, 1977), mixed exponential distribution (Woolhiser and Pegram, 1979) and transformed normal distribution (Bardossy and Plate, 1992).

One commonly used continuous distribution for precipitation data is the gamma distribution, whose probability density function (PDF) is:

$$f(x) = \frac{(x/\beta)^{\alpha-1} \exp(-x/\beta)}{\beta \Gamma(\alpha)} \quad x, \alpha, \beta > 0 \quad \text{Equation 1}$$

The gamma distribution is a two-parameter controlled distribution. These two parameters are  $\alpha$ , the shape parameter; and  $\beta$ , the scale parameter. The density function of the gamma distribution is not analytically integrable. It has to be obtained by computing an approximation of its cumulative distribution function by application of an incomplete gamma function. Therefore, it is relatively computer intensive in comparison with other rainfall generator functions.

The PDF of the gamma distribution possesses a variety of shapes depending on its shape parameter. For the case of  $\alpha = 1$ , the gamma distribution is converted to be another important and relatively simple model for precipitation. This special case is called an exponential distribution, with a PDF:

$$f(x) = \frac{1}{\mu} \exp\left(-\frac{x}{\mu}\right) \quad x, \mu > 0 \quad \text{Equation 2}$$

The exponential distribution has only one parameter,  $\mu$ , the expectation of precipitation amount.

When  $\alpha$  approaches very large value, the shape of the gamma distribution resembles a normal distribution, generally called as gaussian distribution, with a PDF:

$$f(x) = \frac{1}{\sigma \sqrt{2\pi}} \exp\left[-\frac{(x-\mu)^2}{2\sigma^2}\right] \quad \sigma > 0 \quad \text{Equation 3}$$

The Gaussian distribution has many advantages over other distributions. In general, the multivariate distribution is presented by a normal distribution. This is because when the joint distribution is normally distributed, both the conditional distribution and marginal distributions of the univariate are normally distributed as well, which simplifies the problem and makes the model easier to couple with other normally distributed parameters. Multivariate normal distribution can also be applied for describing precipitation, though precipitation is non-symmetrically distributed. The power transformation is required to correct the skewness to mathematically fit to the Gaussian distribution. (Bardossy and Plate, 1992).

As a result, the skewed normal distribution and exponential distribution are chosen for fitting rainfall time series to represent the statistic properties of precipitation.

The distribution of the daily rainfall amount at the location  $u$  is always CP dependent, expressed as  $Z(t, u)$  in **Eq. 4**. It is represented as  $Z^n(t, u)$  and  $Z^e(t, u)$  in the normal distribution and exponential distribution respectively. See **Eq. 5** and **Eq. 6**.

$$P\left[Z(t, u) < z \mid \tilde{A} = \alpha_i, Z(t, u) > 0\right] = F_i(z \mid u) \quad \text{Equation 4}$$

**Normal distribution:**

$$Z^n(t, u) = \begin{cases} 0 & \text{if } W^n(t, u) \leq 0 \\ W^n(t, u)^\beta & \text{if } W^n(t, u) > 0 \end{cases} \quad \text{Equation 5}$$

Here,

- $Z^n(t, u)$ : Daily precipitation amount at time  $t$  and location  $u$
- $W^n(t, u)$ : Normally distributed random variable for location  $u$  at time  $t$
- $\beta$ : Transformation exponent relating  $Z(t, u)$  to  $W(t, u)$

**Exponential distribution:**

$$Z^e(t, u) = \begin{cases} 0 & \text{if } W^e(t, u) \leq p_0(u) \\ -\mu(t, u) * \ln(1 - W^e(t, u)) & \text{if } W^e(t, u) > p_0(u) \end{cases} \quad \text{Equation 6}$$

Here,

- $Z^e(t, u)$ : Daily precipitation amount at time  $t$  and location  $u$
- $W^e(t, u)$ : Uniformly distributed random variable for location  $u$  at time  $t$
- $p_0(u)$ : Probability of precipitation at location  $u$
- $\mu(t, u)$ : Expectation of precipitation at location  $u$

The quasi-linear relationship between the precipitation and moisture flux is first assumed and verified by preliminary analysis for the study area. Under this assumption, the parameters of distribution are represented as  $\mu_i$  in addition to CP-dependent  $\mu_0$  and its annual cycle can be approximately described by the Fourier series. See **Eq. 7** and **Eq. 8**.

$$\mu(t, u) = \mu_0 + a * MF(t, u) \quad \text{Equation 7}$$

$$\mu_i(t^*, u) = \frac{a_0(i, u)}{2} + \sum_{k=1}^K (a_k(i, u) \cos(kwt^*) + b_k(i, u) \sin(kwt^*)) \quad \text{Equation 8}$$

Where  $t^*$  stands for the Julian date correspondent to every actual day;  $\mu_i(t^*, u)$  is the expectation of precipitation on the Julian date presented by the Fourier series.  $a_k$  and  $b_k$  are the coefficients of harmonics of the Fourier series conditioned to CP pattern  $i$ . According to the harmonic analysis, the Fourier approximation is able to be identical with observed time series in case that  $t^*/2$  harmonics are introduced.

The spatial structure of rainfall is presented by a spatial covariance structure  $\Gamma_{0i}(t^*)$  and  $\Gamma_{1i}(t^*)$ , which take spatial covariance and auto-correlation into account

The covariance structure is calculated by **Eq. 9**, where  $p_i$  and  $q_i$  are the circulation pattern dependent and annual dependent parameters described by the Fourier series.  $h(x, y)$  is distance between a pair of stations (Stehlik and Bardossy, 2002).

$$\text{cov}[Z_x, Z_y]_{i(t)} = p_i(t^*) e^{-h(x, y) q_i(t^*)} \quad \text{Equation 9}$$

With introduction of a random number, the precipitation can be generated day by day using the following generating process:

$$W(t) = r(t^*)(W(t-1)) + C_i(t^*)\psi(t) \quad \text{Equation 10}$$

Where,  $t^*$  denotes the Julian date with respect to the consideration of annual impact.  $r(t^*)$  is autocorrelation of a one-day lag to account for the previous day's impact.  $\psi(t)$  is a random number  $N(0, 1)$ .  $C_i(t^*)$  holds for spatial variability.

Similar to precipitation downscaling, the **temperature** generator model is also a CP conditioned downscaling model. Specific circulation patterns are classified prior to the downscaling procedure. The auto-regressive moving average method is applied to set up the model to generate daily temperatures, which is a function of geopotential height at daily temporal resolution.

Instead of SLP, geopotential height at 700 hpa is used as an indicator, together with temperature related objective function for CP classification.

## 4 Result

### 4.1 Precipitation downscaling model

#### 4.1.1 Performance of classified circulation patterns

From a statistical point of view, time series of observations should be as long as possible. Constrained by data availability, the station Tashkent is the only one that has long term measurements in terms of both precipitation and temperature, more than a hundred years. For this reason, daily precipitation and daily maximum and minimum temperatures were individually used as local variables for optimizing precipitation CPs and temperature CPs.

The CPs for the Chirchik-Ahangaran river basin are generated by using normalized pressure anomalies of sea level pressure (SLP) derived from the NCEP reanalysis data set at a spatial resolution of 2.5° X 2.5° covering Central Asia windows.

The circulation patterns consist of total 12 types and some of them dominate specific climate conditions. The anomaly maps of single CPs are presented in **Appendix I**.

The behavior of local rainfall events in relation to the governing CPs is identified using the index “Wetness” which describes the contribution of a certain CP to precipitation. The wetness can be valued as 1, <1 and >1 indicating normal, dry and wet respectively. The larger the wetness, the wetter the CP is and vice versa.

The figure below shows that CP08 and CP11 can be apparently recognized as wet CPs no matter whether in winter or summer, while CP02, CP03 and CP10 are quite dry.

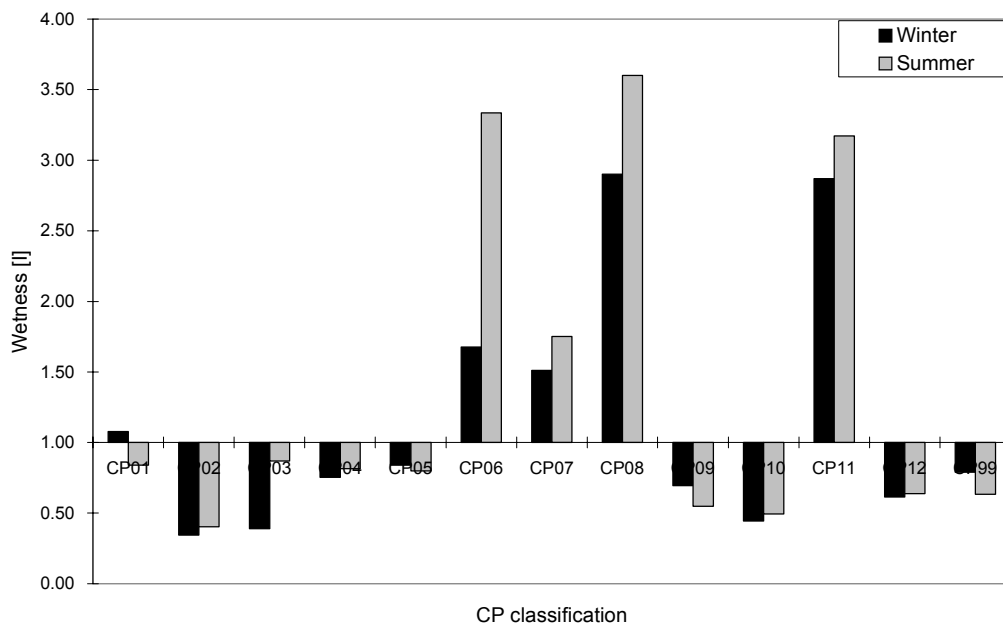


**Figure 4: Wetness of individual CPs classified for Chirchik-Ahangaran regions**

Several statistical indices are defined and calculated to compare the contribution of CPs to the rainfall from season to season. These indices are CP-Frequency, CP-Mean, CP-90. CP-Frequency presents the partition of a particular CP occurred during the studying time slice; CP-Mean calculates for the contribution of each CP to average rainfall and last index stands

for that to rainfall under extreme event that is defined as rainfall larger than 90<sup>th</sup> percentile of total rainfall. The results are listed in the following tables. [Tab. 4-7]

Combining this with results shown in Fig. 4, the same conclusion can be drawn out. With regards to CP08 and CP11, their low pressure zones cover most part of Kyrgyzstan and Tadzhikistan and the western range of the Tiangshan Mountains and therefore cause a high amount rainfall, though occur infrequently. Both of them contribute to most rainfall events, especially to extreme cases. This is why they are named “wet CPs”. In contrast to “wet CPs”, CP02 and CP10 are clearly two “dry CPs”. They occur frequently, but their contribution to rainfall processes is very limited due to high pressure zone dominating regions.

The contribution of single CP to rainfall events is chosen as criterion to reclassify CPs. Thereafter, the variability of precipitation conditioned to each group of CPs is captured by distribution functions and daily precipitation is generated stochastically, together with consideration of spatial correlation amongst stations and auto-correlation at each single station.

**Table 4: Frequency and amount of precipitation conditioned to CPs [spring]**

|      | <b>CP-Frequency [%]</b> | <b>CP-Mean [%]</b> | <b>CP-90 [%]</b> |
|------|-------------------------|--------------------|------------------|
| CP01 | 5.10                    | 3.0                | 3.5              |
| CP02 | 13.5                    | 5.1                | 3.5              |
| CP03 | 4.4                     | 2.0                | 0.3              |
| CP04 | 12.6                    | 11.6               | 6.7              |
| CP05 | 5.3                     | 4.2                | 3.7              |
| CP06 | 4.0                     | 8.2                | 7.8              |
| CP07 | 3.8                     | 4.8                | 5.3              |
| CP08 | <b>5.9</b>              | <b>14.1</b>        | <b>23.2</b>      |
| CP09 | 10.7                    | 9.4                | 8.8              |
| CP10 | 8.6                     | 5.2                | 3.9              |
| CP11 | <b>6.9</b>              | <b>17.3</b>        | <b>28.9</b>      |
| CP12 | 7.5                     | 7.0                | 2.3              |

**Table 5: Frequency and amount of precipitation conditioned to CPs [summer]**

|      | <b>CP-Frequency [%]</b> | <b>CP-Mean [%]</b> | <b>CP-90 [%]</b> |
|------|-------------------------|--------------------|------------------|
| CP01 | 7.4                     | 5.9                | 5.9              |
| CP02 | 13.4                    | 1.8                | 0.0              |
| CP03 | 5.9                     | 6.4                | 7.4              |
| CP04 | 13.1                    | 11.9               | 7.6              |
| CP05 | 7.8                     | 10.7               | 5.6              |
| CP06 | 3.3                     | 4.3                | 4.5              |
| CP07 | 4.2                     | 6.8                | 8.3              |
| CP08 | <b>3.5</b>              | <b>18.5</b>        | <b>48.0</b>      |
| CP09 | 12.6                    | 6.7                | 1.1              |
| CP10 | 8.1                     | 5.2                | 2.8              |
| CP11 | <b>3.9</b>              | <b>9.7</b>         | <b>4.5</b>       |
| CP12 | 7.3                     | 4.8                | 2.5              |

**Table 6: Frequency and amount of precipitation conditioned to CPs [autumn]**

|      | <b>CP-Frequency [%]</b> | <b>CP-Mean [%]</b> | <b>CP-90 [%]</b> |
|------|-------------------------|--------------------|------------------|
| CP01 | 5.2                     | 4.5                | 3.9              |
| CP02 | 15.9                    | 3.1                | 1.0              |
| CP03 | 5.0                     | 0.9                | 1.6              |
| CP04 | 13.3                    | 14.5               | 7.0              |
| CP05 | 5.9                     | 3.4                | 1.4              |
| CP06 | 3.1                     | 7.7                | 12.3             |
| CP07 | 3.2                     | 2.4                | 5.5              |
| CP08 | <b>4.4</b>              | <b>12.2</b>        | <b>20.5</b>      |
| CP09 | 10.2                    | 7.4                | 1.4              |
| CP10 | 7.5                     | 2.3                | 0.0              |
| CP11 | <b>5.8</b>              | <b>22.7</b>        | <b>33.9</b>      |
| CP12 | 8.5                     | 7.4                | 3.3              |

**Table 7: Frequency and amount of precipitation conditioned to CPs [winter]**

|      | <b>CP-Frequency [%]</b> | <b>CP-Mean [%]</b> | <b>CP-90 [%]</b> |
|------|-------------------------|--------------------|------------------|
| CP01 | 3.6                     | 4.3                | 1.4              |
| CP02 | 14.8                    | 3.1                | 0.4              |
| CP03 | 4.4                     | 2.9                | 2.3              |
| CP04 | 14.6                    | 14.8               | 19.6             |
| CP05 | 7.1                     | 3.2                | 0.8              |
| CP06 | 4.3                     | 10.5               | 11.1             |
| CP07 | 4.0                     | 4.4                | 3.3              |
| CP08 | <b>3.4</b>              | <b>6.3</b>         | <b>11.0</b>      |
| CP09 | 9.0                     | 6.4                | 2.6              |
| CP10 | 8.3                     | 5.9                | 2.5              |
| CP11 | <b>8.4</b>              | <b>21.0</b>        | <b>32.2</b>      |
| CP12 | 7.6                     | 6.7                | 5.7              |

The contribution of a single CP to rainfall events is chosen as criterion for reclassifying the CPs. Thereafter, the variability of precipitation conditioned to each group of CPs is captured by distribution functions and daily precipitation is generated stochastically, together with consideration of spatial correlation amongst stations and auto-correlation at each single station.

#### **4.1.2 Impact of moisture flux derived from large-scale parameters**

Additionally, daily moisture flux is incorporated as a potential predictor that has been proved to have a dominant impact on the rainfall process. Zonal wind components are proved again to be dominant for daily precipitation in the Chirchik-Ahangaran river basin.

The impact of moisture flux on local rainfall is analyzed in order to determine the most dominant factors. Based on knowledge, the moisture flux may be carried by wind from the Atlantic Ocean from the West and the Barents Sea from North. Therefore, moisture flux from both directions at different pressure levels is considered as a potential predictor. Through correlation tests, finally the westerly moisture flux derived from 700 hPa is identified to be the most important factor.

**Table 8: Correlation of local precipitation to moisture flux at different pressure levels**

|         | U – 700      | V – 700 | U - 850 | V - 850 |
|---------|--------------|---------|---------|---------|
| Group 1 | <b>0.417</b> | 0.336   | 0.384   | 0.240   |
| Group 2 | <b>0.266</b> | 0.127   | 0.041   | -0.132  |

### 4.1.3 Calibration and validation of model’s performance

Only 5 stations containing relatively long observation time series can be used for statistical downscaling. These 5 stations are Pskem, Charvak, Tashkent, Paca-ata and Urtatoky, located in the upper chirchik, lower chirchik and in the mountains area in Kyrgyzstan respectively. Due to a limitation of data availability, daily time series measured at those stations from the year 1960 to 1976 are using for the model’s calibration and the monthly rainfall amount for the other years provided by Uzbekistan partners are used for validation.

Two model settings incorporated with moisture flux are using here, one is presented with a skewed normal distribution and the other is with an exponential distribution.

Firstly, the annual cycle of each station is compared with that derived from observation. Observed and simulated average monthly precipitation is used as the first indicator to demonstrate the model’s performance. The aim is to capture the monthly mean value, which is important for long-term analysis. The result of the comparison is presented in the following figures. [Fig. 5 – Fig. 9]

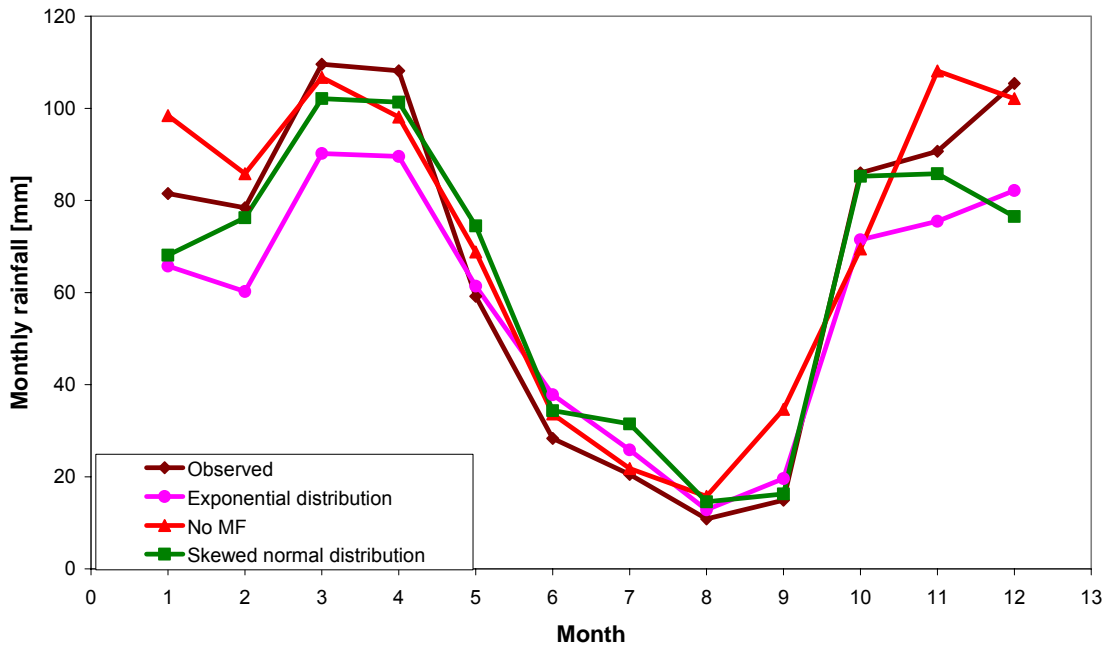


**Figure 5: Annual cycle of monthly precipitation derived from observation and simulation out of 2 model settings during calibration [Station: Pskem]**

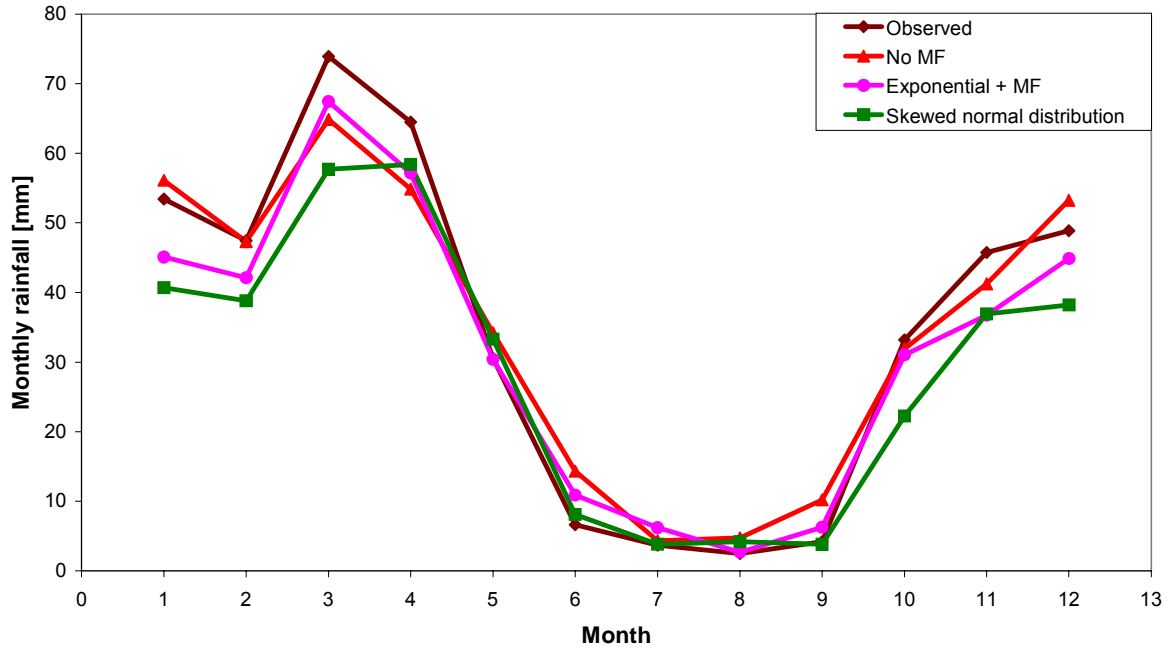


**Figure 6:** Annual cycle of monthly precipitation derived from observation and simulation out of 2 model settings during calibration [Station: Tashkent]

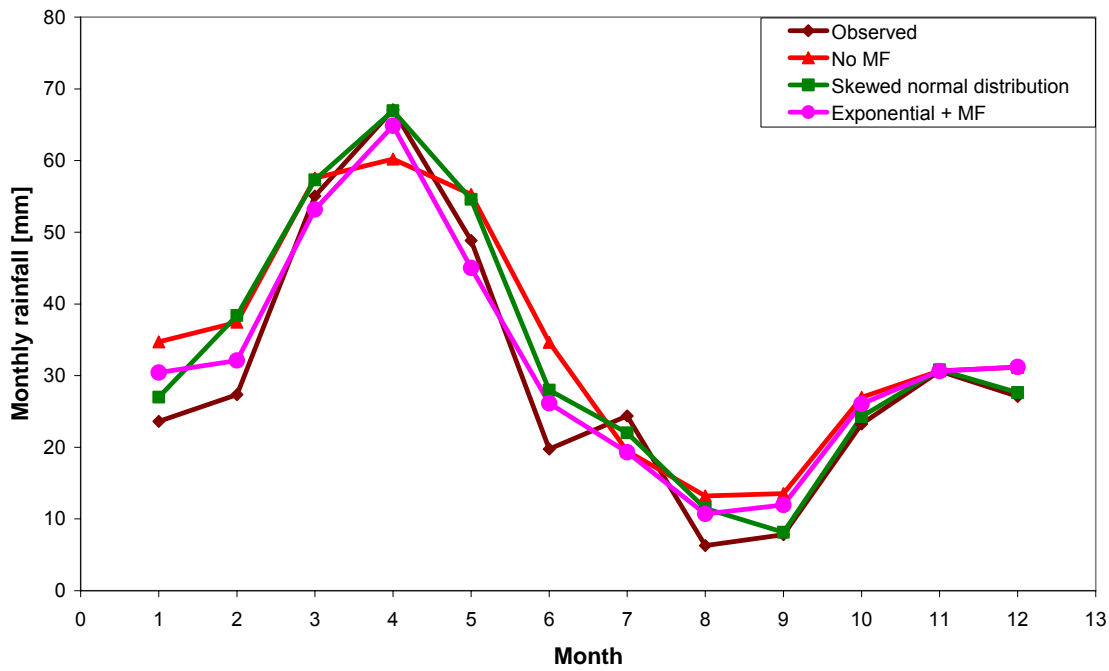


**Figure 7:** Annual cycle of monthly precipitation derived from observation and simulation out of 2 model settings during calibration [Station: Urtatoky]

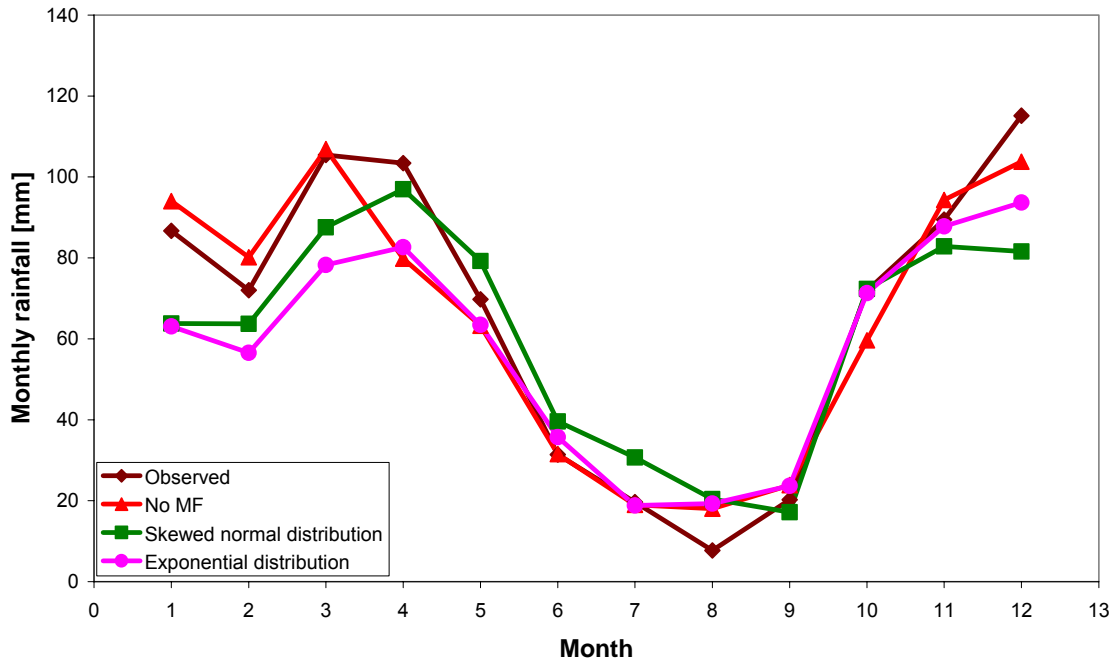


**Figure 8:** Annual cycle of monthly precipitation derived from observation and simulation out of 2 model settings during validation [Station: Pskem]

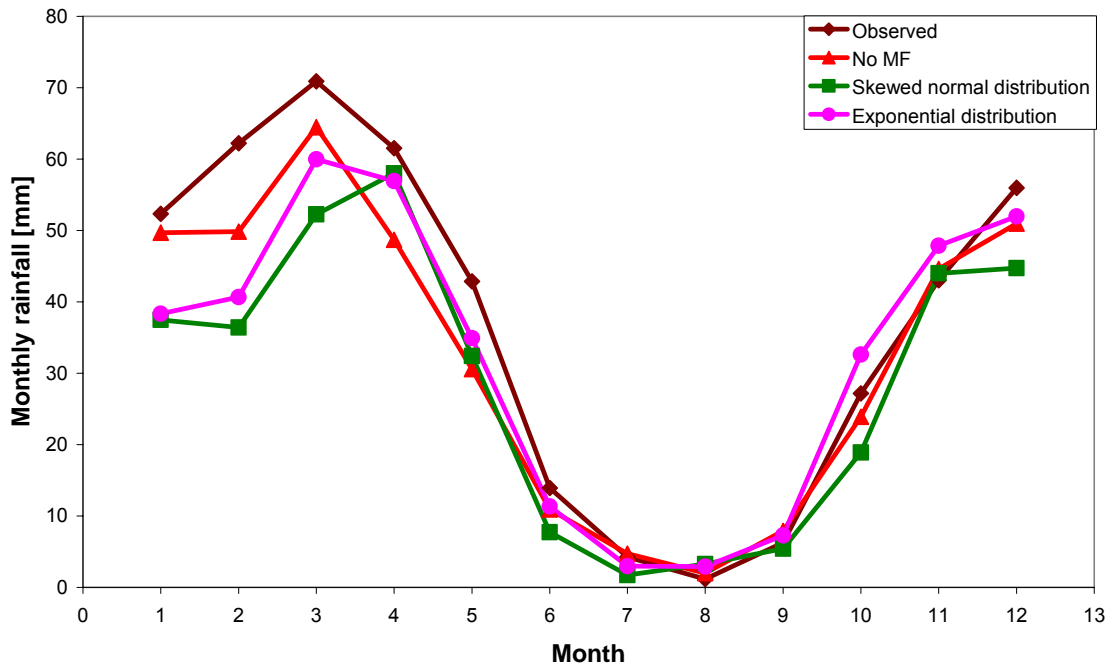


**Figure 9:** Annual cycle of monthly precipitation derived from observation and simulation out of 2 model settings during validation [Station: Tashkent]

The output of both model settings turned out to be successful in capturing monthly mean precipitations that is consistent with observations. All the simulations represent the occurrence of peak rainfalls in the spring months, mostly in March and April that is differentiated between plain and mountainous area. However, there is still bias between

monthly precipitation derived from observation and simulations, especially at the beginning of the year.

As well as the long-term mean quite important, the model's performance under extreme conditions is also of great interest. Therefore, the model's capability of representing inter-annual variability is also under evaluation using precipitation related indices, listed in **Tab. 9**.

**Table 9: Diagnostic indices for long-term precipitation**

| Precipitation related indices |   |
|-------------------------------|---|
| Pav [mm/day]                  | Average precipitation   |
| P90 [mm/day]                  | 90 <sup>th</sup> percentile of rainy day's amounts                      |
| 90T                           | % of total rainfall from events > long-term 90 <sup>th</sup> percentile |
| 90N                           | No. of events > long-term 90 <sup>th</sup> percentile of rainy days     |

**Table 10: Precipitation related diagnostic analysis in winter and summer**

|     |                      | Winter |             |      | Summer |             |       |
|-----|----------------------|--------|-------------|------|--------|-------------|-------|
|     |                      | Bias   | Correlation |      | Bias   | Correlation |       |
|     |                      | Aver   | Max         | Aver | Aver   | Max         | Aver  |
| Pav | CP + MF <sup>1</sup> | 0.41   | 0.53        | 0.32 | 0.14   | 0.60        | 0.31  |
|     | CP + MF <sup>2</sup> | 0.35   | 0.75        | 0.48 | 0.13   | 0.60        | 0.35  |
| 90T | CP + MF <sup>1</sup> | 0.04   | 0.38        | 0.09 | 0.05   | 0.37        | 0.06  |
|     | CP + MF <sup>2</sup> | 0.03   | 0.37        | 0.07 | 0.05   | 0.37        | 0.07  |
| 90N | CP + MF <sup>1</sup> | 0.42   | 0.44        | 0.17 | 0.16   | 0.45        | 0.11  |
|     | CP + MF <sup>2</sup> | 0.28   | 0.50        | 0.21 | 0.20   | 0.42        | 0.15  |
| P90 | CP + MF <sup>1</sup> | 2.48   | 0.40        | 0.12 | 3.08   | 0.34        | -0.07 |
|     | CP + MF <sup>2</sup> | 2.86   | 0.52        | 0.13 | 3.22   | 0.59        | 0.15  |

**Table 11: Precipitation related diagnostic analysis in spring and autumn**

|     |                      | Spring |             |      | Autumn |             |      |
|-----|----------------------|--------|-------------|------|--------|-------------|------|
|     |                      | Bias   | Correlation |      | Bias   | Correlation |      |
|     |                      | Aver   | Max         | Aver | Aver   | Max         | Aver |
| Pav | CP + MF <sup>1</sup> | 0.20   | 0.63        | 0.41 | 0.15   | 0.64        | 0.29 |
|     | CP + MF <sup>2</sup> | 0.31   | 0.72        | 0.53 | 0.14   | 0.65        | 0.43 |
| 90T | CP + MF <sup>1</sup> | 0.03   | 0.46        | 0.12 | 0.06   | 0.34        | 0.05 |
|     | CP + MF <sup>2</sup> | 0.03   | 0.37        | 0.08 | 0.05   | 0.35        | 0.04 |
| 90N | CP + MF <sup>1</sup> | 0.33   | 0.49        | 0.22 | 0.21   | 0.45        | 0.15 |
|     | CP + MF <sup>2</sup> | 0.24   | 0.54        | 0.25 | 0.21   | 0.50        | 0.21 |
| P90 | CP + MF <sup>1</sup> | 1.39   | 0.45        | 0.17 | 1.80   | 0.48        | 0.08 |
|     | CP + MF <sup>2</sup> | 2.33   | 0.45        | 0.17 | 2.60   | 0.62        | 0.12 |

As shown by diagnostic analysis, [**Tab. 10** and **Tab. 11**], the model performs well with respect to average precipitation "Pav" in most seasons even in summer. The average correlation between simulated and observed precipitation reaches a high value of 0.53 in spring and a lowest value of 0.35 in summer. For the other indices, the average correlation is not as high as Pav, but they still reach an acceptable level in extreme conditions. However, the model is quite weak in representing the percentage of total rainfall from events whose amount is higher than the long-term 90<sup>th</sup> percentile.

<sup>1</sup> Model setting with skewed normal distribution

<sup>2</sup> Model setting with exponential distribution

Generally speaking, our model is able to describe inter-annual variability of precipitation at a seasonal scale. All indices achieve the highest correlation in spring, even for extreme indices, followed by the winter, autumn and summer. Compared with the skewed normal distribution, the setting with an exponential distribution is better, especially under extremes. Therefore, the further downscaling will adopt an exponential distribution to describe precipitation time series.

#### 4.1.4 Climate scenarios

In order to study climate condition under impact of climate change, the large-scale parameters derived from A2 and B2 ensembles provided by global circulation models (GCMs) are downscaled for target regions for the first 30 years of the current century, from the year 2000 to 2030. In this paper, ECHAM 4, developed by the Max-Planck Institute in Hamburg is chosen to provide climate information at a large-scale. Its model output from the control run is used to evaluate the predictor used for the downscaling process and its output conditioned to A2 and B2 scenarios are used to downscale daily precipitation and temperature.

The circulation patterns for precipitation and temperature for the time period up to the year 2030 are derived from mean sea level pressure and geopotential height (700 hpa level) from the ECHAM4 output. The mean seasonal frequency and mean persistence of specific precipitation CPs are compared between NCEP derived CPs and ECHAM4 derived CPs. See **Tab. 12** to **Tab. 17**.

**Table 12: Frequency of precipitation CPs in winter and summer [%]**

|      | Winter |                  |      |      | Summer |                  |      |      |
|------|--------|------------------|------|------|--------|------------------|------|------|
|      | NCEP   | CTL <sup>3</sup> | A2   | B2   | NCEP   | CTL <sup>3</sup> | A2   | B2   |
| CP08 | 3.49   | 4.06             | 5.66 | 5.70 | 3.81   | 3.99             | 7.12 | 7.40 |
| CP02 | 14.5   | 15.8             | 14.8 | 15.5 | 13.70  | 14.3             | 9.44 | 10.1 |

**Table 13: Frequency of precipitation CPs in spring and autumn [%]**

|      | Spring |                  |      |      | Autumn |                  |      |      |
|------|--------|------------------|------|------|--------|------------------|------|------|
|      | NCEP   | CTL <sup>3</sup> | A2   | B2   | NCEP   | CTL <sup>3</sup> | A2   | B2   |
| CP08 | 5.77   | 4.31             | 5.47 | 6.16 | 4.30   | 3.80             | 6.06 | 6.31 |
| CP02 | 13.90  | 15.0             | 17.2 | 17.7 | 16.20  | 16.30            | 13.7 | 13.9 |

**Table 14: Mean persistence of precipitation CPs in winter and summer [day]**

|      | Winter |                  |      |      | Summer |                  |      |      |
|------|--------|------------------|------|------|--------|------------------|------|------|
|      | NCEP   | CTL <sup>3</sup> | A2   | B2   | NCEP   | CTL <sup>3</sup> | A2   | B2   |
| CP08 | 1.09   | 1.35             | 1.31 | 1.14 | 1.30   | 1.18             | 1.42 | 1.46 |
| CP02 | 1.72   | 2.18             | 2.02 | 1.95 | 2.05   | 1.88             | 1.74 | 1.69 |

**Table 15: Mean persistence of precipitation CPs in spring and autumn [day]**

|      | Spring |                  |      |      | Autumn |                  |      |      |
|------|--------|------------------|------|------|--------|------------------|------|------|
|      | NCEP   | CTL <sup>3</sup> | A2   | B2   | NCEP   | CTL <sup>3</sup> | A2   | B2   |
| CP08 | 1.24   | 1.12             | 1.27 | 1.23 | 1.22   | 1.33             | 1.23 | 1.20 |
| CP02 | 2.02   | 1.86             | 2.09 | 2.16 | 2.34   | 1.95             | 1.94 | 1.88 |

<sup>3</sup> Circulation patterns derived from ECHAM4's control run

**Table 16: Maximum persistence of precipitation CP in winter and summer [day]**

|      | Winter |                  |    |    | Summer |                  |    |    |
|------|--------|------------------|----|----|--------|------------------|----|----|
|      | NCEP   | CTL <sup>3</sup> | A2 | B2 | NCEP   | CTL <sup>3</sup> | A2 | B2 |
| CP08 | 2      | 8                | 5  | 3  | 3      | 4                | 6  | 6  |
| CP02 | 7      | 10               | 7  | 10 | 6      | 9                | 10 | 8  |

**Table 17: Maximum persistence of precipitation CP in spring and autumn [day]**

|      | Spring |                  |    |    | Autumn |                  |    |    |
|------|--------|------------------|----|----|--------|------------------|----|----|
|      | NCEP   | CTL <sup>3</sup> | A2 | B2 | NCEP   | CTL <sup>3</sup> | A2 | B2 |
| CP08 | 4      | 4                | 4  | 4  | 3      | 4                | 4  | 3  |
| CP02 | 7      | 8                | 11 | 13 | 12     | 7                | 9  | 7  |

Of all the seasons, spring and summer are of most interest. For spring, both of the frequencies of wet and dry CPs derived from scenarios are higher than those derived from a control run. Meanwhile, the mean and maximum persistences of particular CPs are also higher. For summer, the wet CP is supposed to occur more frequently together with relatively longer persistence and the dry CP with less frequency and shorter persistence, indicating that the wetter climate condition in summer may be noticed in the future.

In addition, the uncertainty of the moisture flux derived from the global model is also under investigation. In the following figure, it can be seen that the modeled moisture flux from the control run of the GCM is slightly underestimated compared with that from assimilation model of NCEP. Considering the consistence of the model itself, the generated scenarios will carry the model's uncertainty and cause an underestimation of moisture flux in the future that may lead to estimation of fewer precipitations in the future.

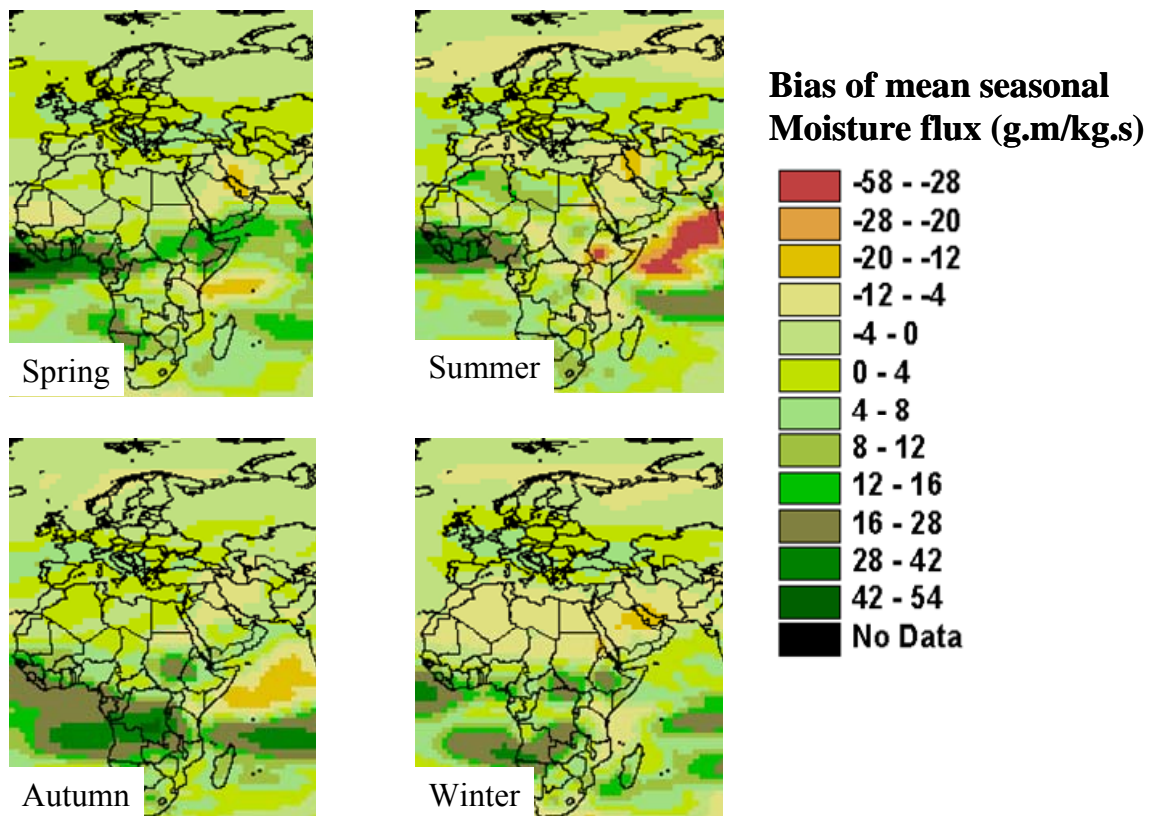


**Figure 10: Comparison between moisture flux derived from NCEP and GCM [Positive: GCM larger than NCEP; Negative: GCM smaller than NCEP]**

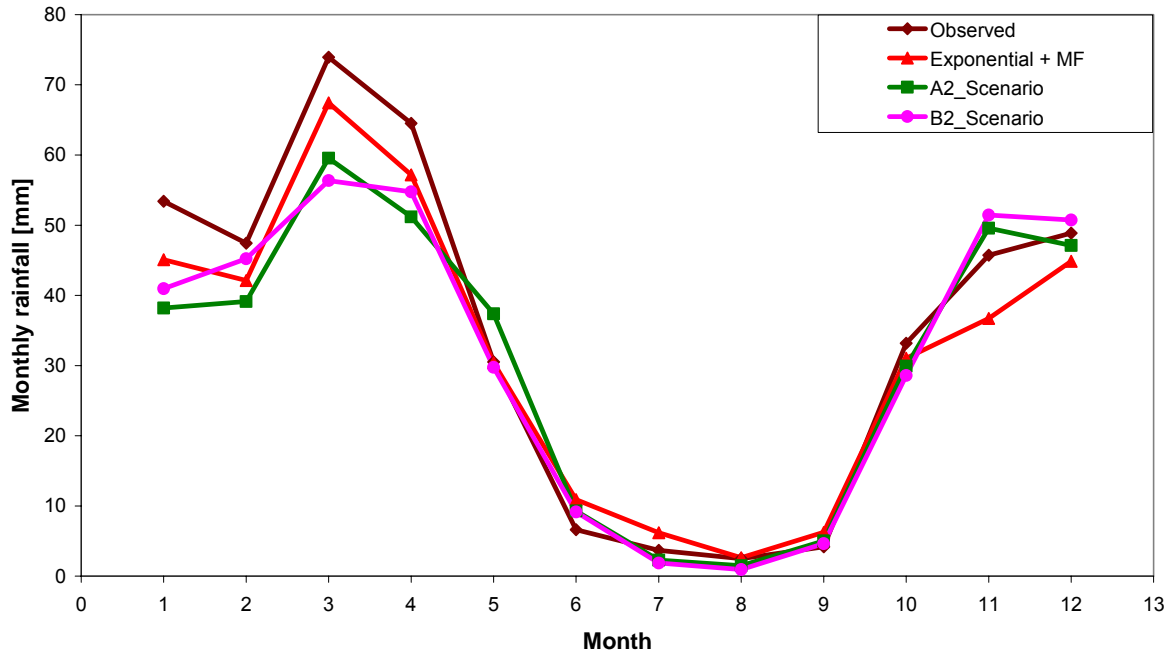


**Figure 11:** Comparison between observed, simulated of current climate and that in future based on ECHAM4 scenarios A2 and B2 [Station: Tashkent]

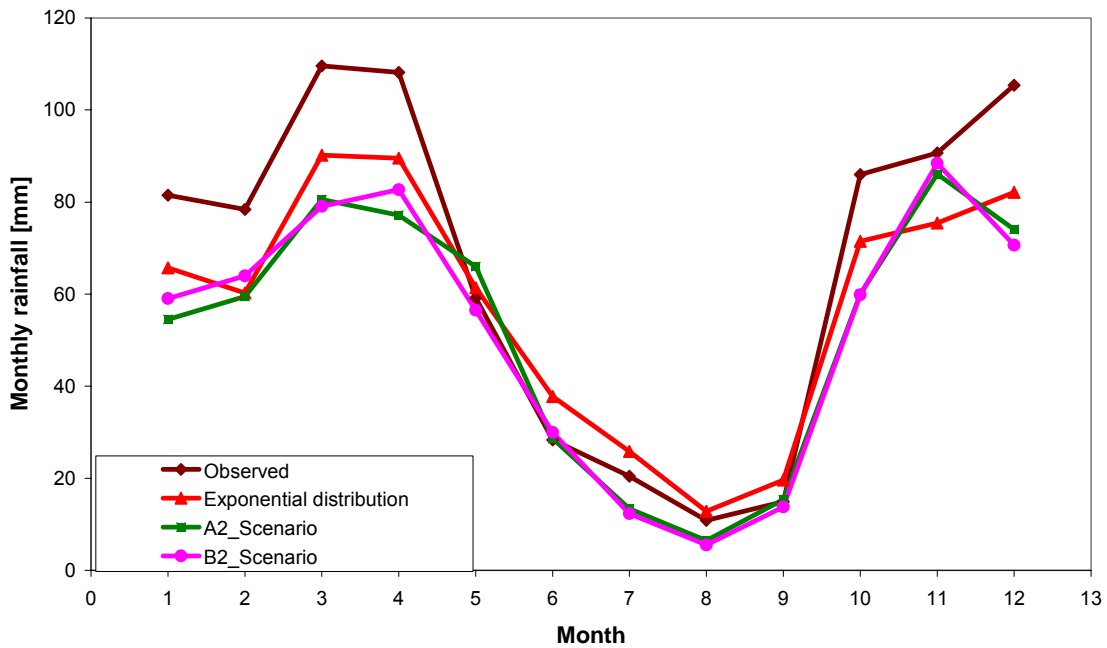


**Figure 12:** Comparison between observed, simulated of current climate and that in future based on ECHAM4 scenarios A2 and B2 [Station: Pskem]

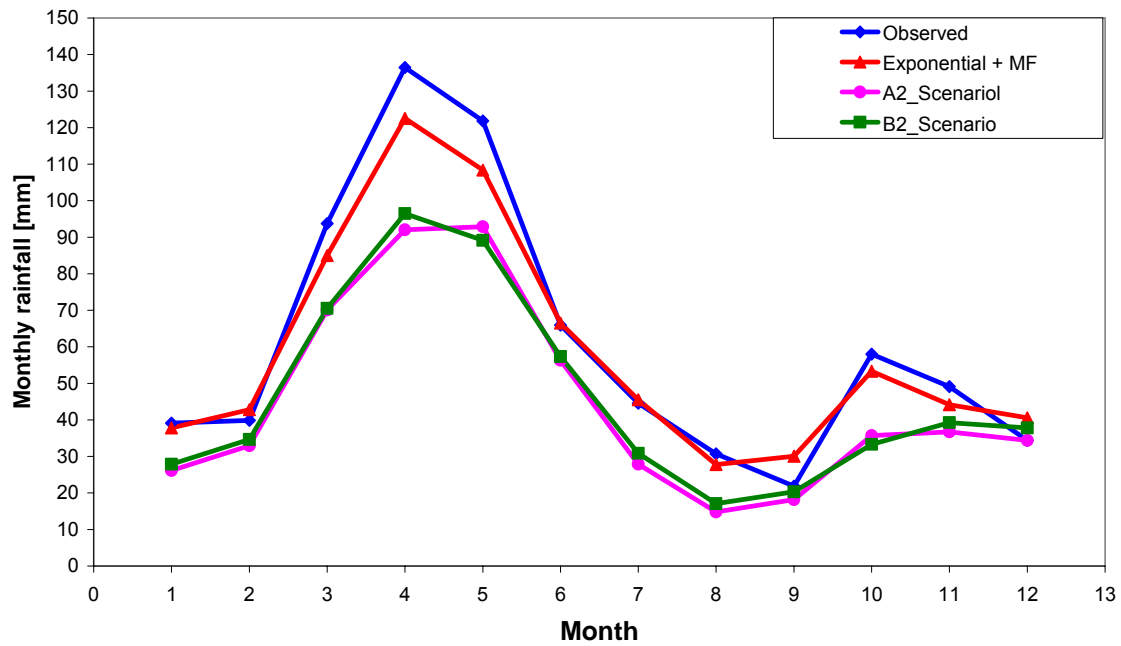


**Figure 13: Comparison between observed, simulated of current climate and that in future based on ECHAM4 scenarios A2 and B2 [Station: Paca – ata]**

Finally, as an integrated response to both CPs and moisture flux, the annual cycle of monthly precipitation derived from the A2 and B2 scenarios point out that in the future both spring and summer are likely to be relatively drier, especially in mountainous area in Kirgizstan part.

## 4.2 Temperature downscaling model

### 4.2.1 Performance of classified circulation patterns

Daily maximum and daily minimum temperature measured at the Tashkent station during the period from 1960 to 1990 are used as local variables to classify circulation patterns for the purpose of downscaling temperature related variables.

Twelve CPs have been classified, showing the different behavior of temperature under the impact of circulation patterns. The average annual cycle derived from conditional and unconditional cases for each station is analyzed to evaluate the performance of the CPs, see **Appendix II**. Of 12 CPs, CP08, CP10 and CP12 are recognized as “warm” CPs, while CP01, CP05 and CP09 are “cold” CPs.

Due to data limitation, there are only 9 stations lasting for 3 years (2001-2003) containing daily minimum and maximum temperature. In order to tackle the problem of short historical time series, the classified CPs are regrouped to be cold CPs, warm CPs, moderate CPs and a non- classified CP, to capture variation.

These 9 stations are distributed over the whole catchment area, their elevations ranging from 477 m on the plain to 2151 m in the mountainous area. The average annual temperature cycle at a single station is generated to validate the model output. For the time period of calibration period, the validation is performed of monthly maximum temperature and minimum temperature derived from simulated time series, compared with that provided by local partners.

### 4.2.2 Validation of model’s performance

There are 5 stations that are quite important for local agriculture. Angren and Tashkent are located on the plain of the lower Chirchik-Ahangaran region, while Dukant, Olgaing and Pskem are lying in the mountainous areas of the upper Chirchik-Ahangaran. Because of difference in elevation, there is quite big difference in the peak value in summer and winter.

There is about 5 °C difference between stations on the plain and in the mountains, that can be demonstrated by comparing station Angren, for example, with station Dukant. See **Fig. 14 – 17**.

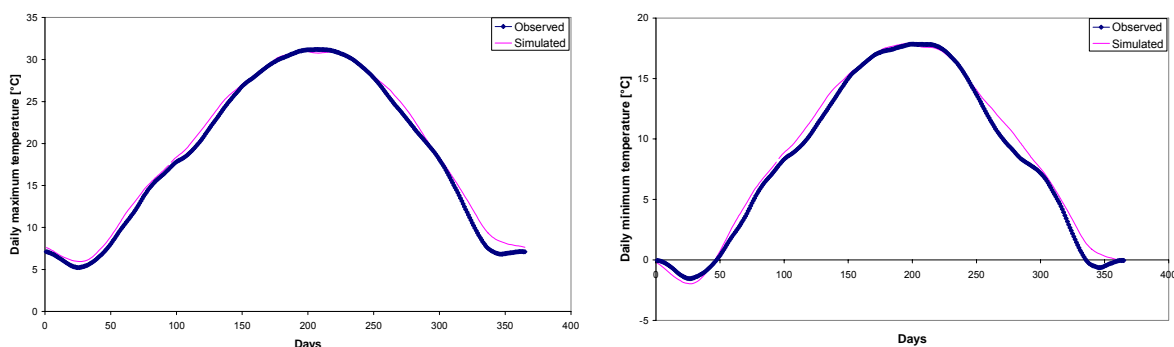


**Figure 14:** Annual cycle of Tmax and Tmin derived from Observed and simulated time series at Station Angren [Left: Tmax; Right: Tmin]

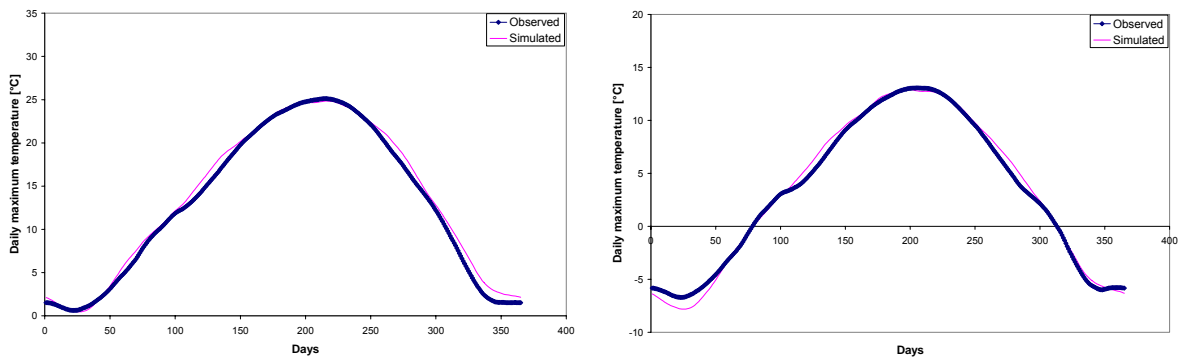


**Figure 15:** Annual cycle of Tmax and Tmin derived from Observed and simulated time series at Station Dukant [Left: Tmax; Right: Tmin]

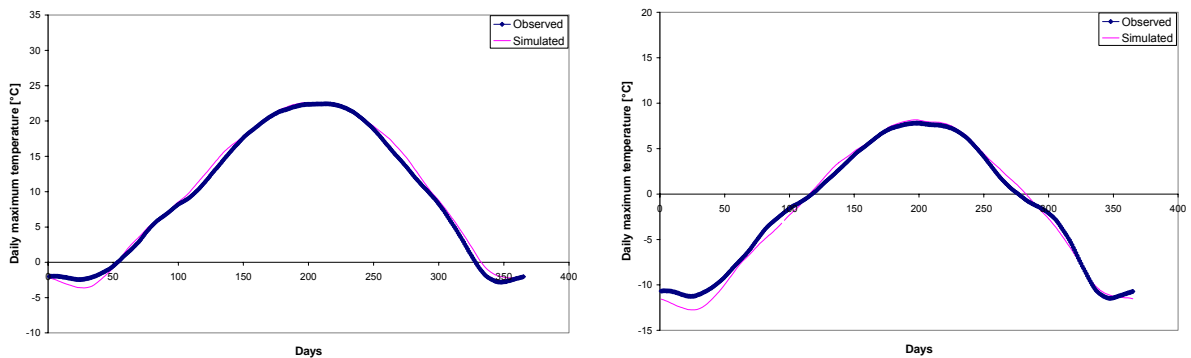


**Figure 16:** Annual cycle of Tmax and Tmin derived from Observed and simulated time series at Station Olgaing [Left: Tmax; Right: Tmin]

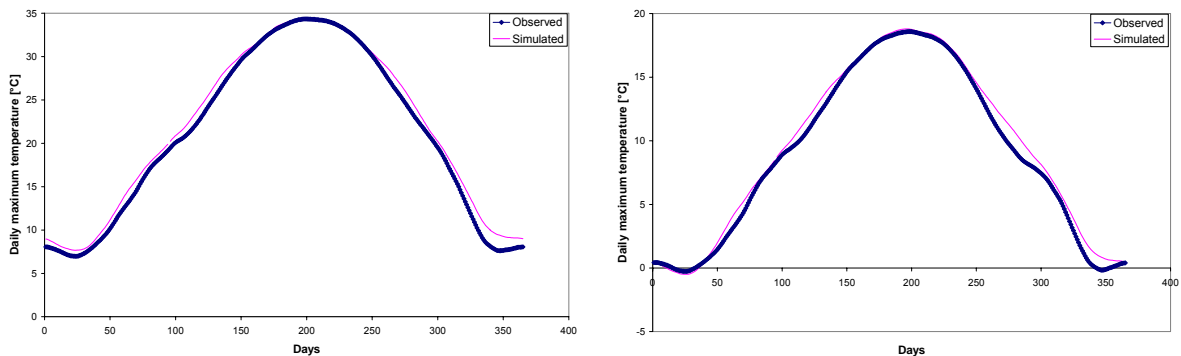


**Figure 17:** Annual cycle of Tmax and Tmin derived from Observed and simulated time series at Station Tashkent [Left: Tmax; Right: Tmin]

Nevertheless, our model output captures aforementioned differences in addition to annual cycle for each station.

Additionally, temperature related diagnostic indices are calculated for the calibration period to evaluate inter-annual variability. The indices used are listed in the table below.

**Table 18:** Diagnostic indices for long-term temperature

| Temperature related indices |                                  |
|-----------------------------|----------------------------------|
| Txav [°C]                   | Average daily Tmax               |
| Tnav [°C]                   | Average daily Tmin               |
| Tmin10 [°C]                 | Tmin 10 <sup>th</sup> percentile |
| Tmax90 [°C]                 | Tmax 90 <sup>th</sup> percentile |

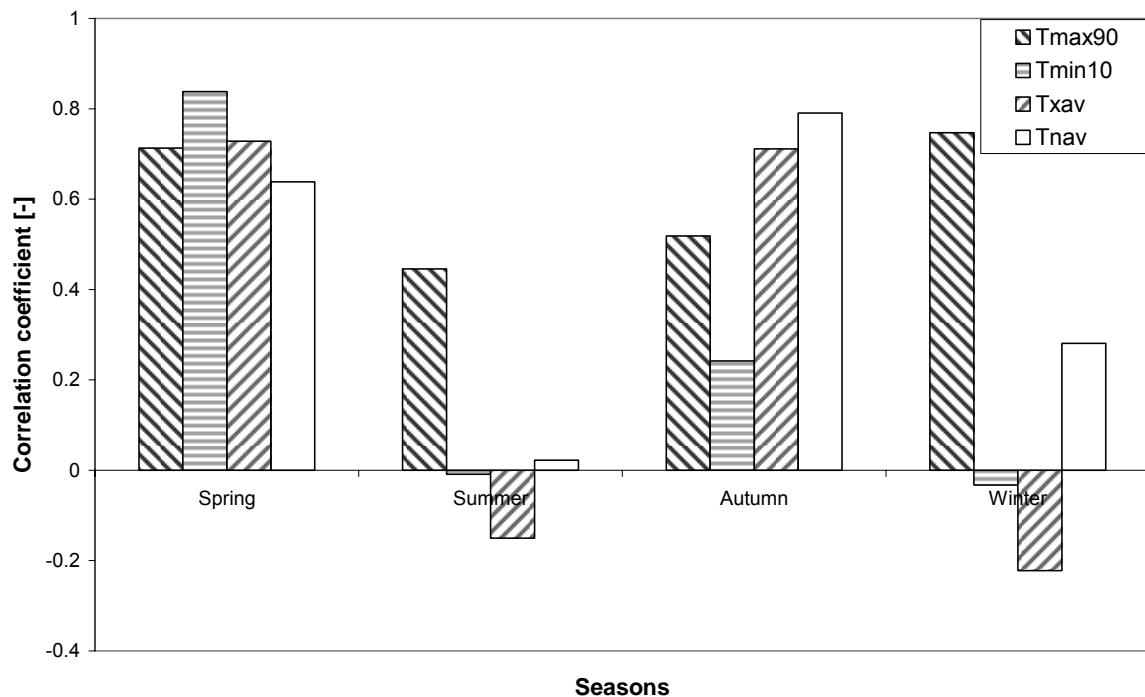


**Figure 18: Temperature related indices over stations in the Chirchik-Ahangaran river basin on a seasonal scale**

The indices are calculated on a seasonal basis and their performance can be viewed in **Fig. 18**.

In the above figure, all indices in spring and autumn reach quite high correlation, while the performance of the model for summer and winter are not consistent for all indices. For summer, the model is able to represent the average daily maximum temperature but is significantly weaker for the other indices. For winter, the model is good at representing the daily maximum and average minimum temperature, but quite unsatisfactory with the other 2 indices.

Unfortunately, there is no available long-term daily time series of observed temperature. The weakness of the model may be caused by the grouping of circulation patterns. The result can be improved when more data sources are available.

However, there are enough consistencies between observed and downscaled meteorological parameters. As a result, our model is further used to generate temperature parameters from the global circulation model (GCM).

#### 4.2.3 Climate scenarios

In the Chirchik – Ahangaran area, the temperatures in spring and summer are quite dominant for local regions, which is limiting factor for critical events like snow melting and heat wave. In comparison to the annual cycle of daily maximum and minimum temperatures derived from global scenarios and observations, it is found that temperature is generally increased over the whole year. But two important increases should be kept in mind: one will occur in February that may cause more snow melting to happen; the other in July,

traditionally the hottest month. Both of them indicate that in the next 30 years there may be longer summers and warmer winters. See **Fig. 19** and **Fig. 20**.

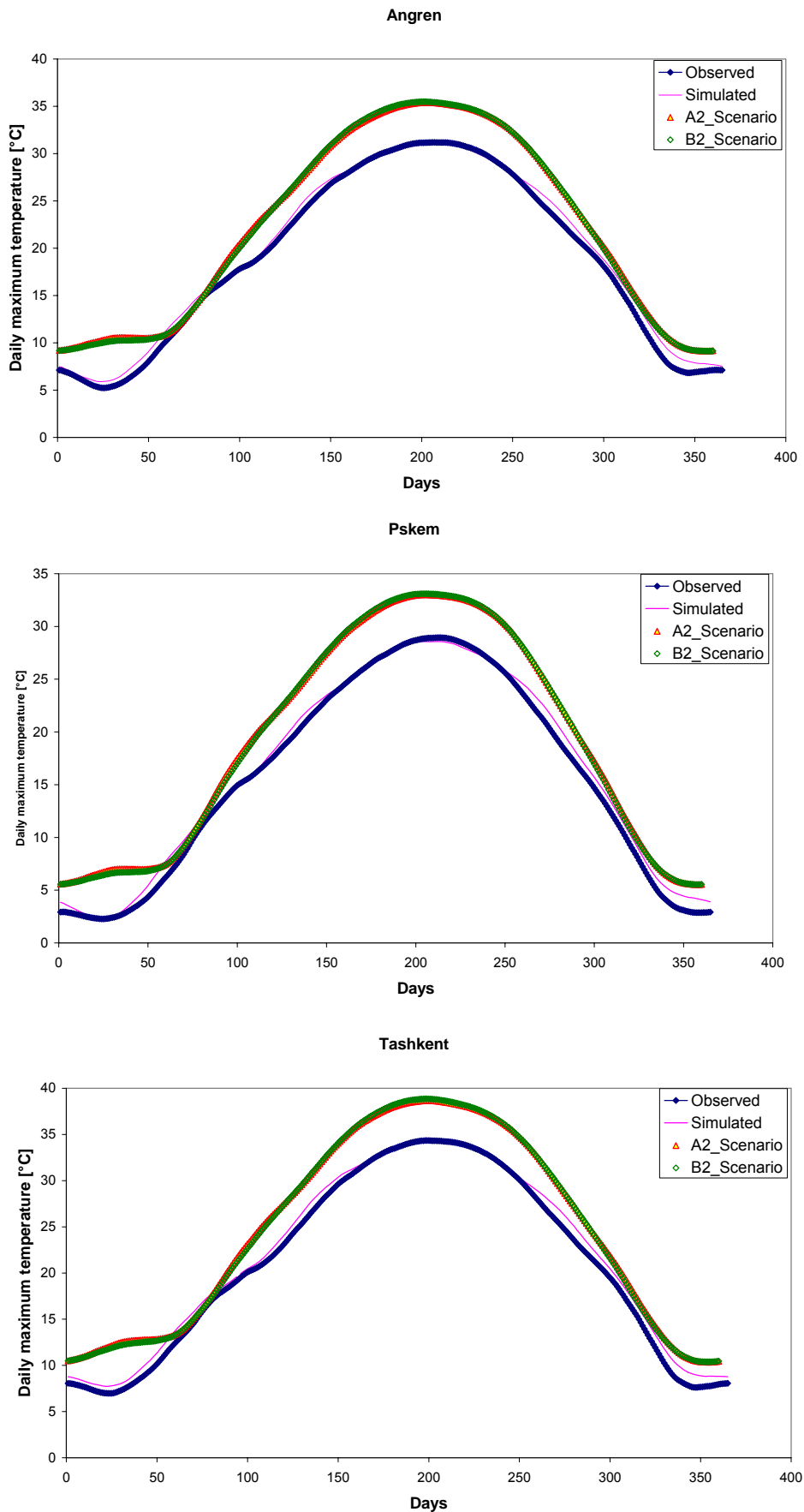


**Figure 19:** Downscaled daily maximum temperature derived from A2 and B2 scenarios

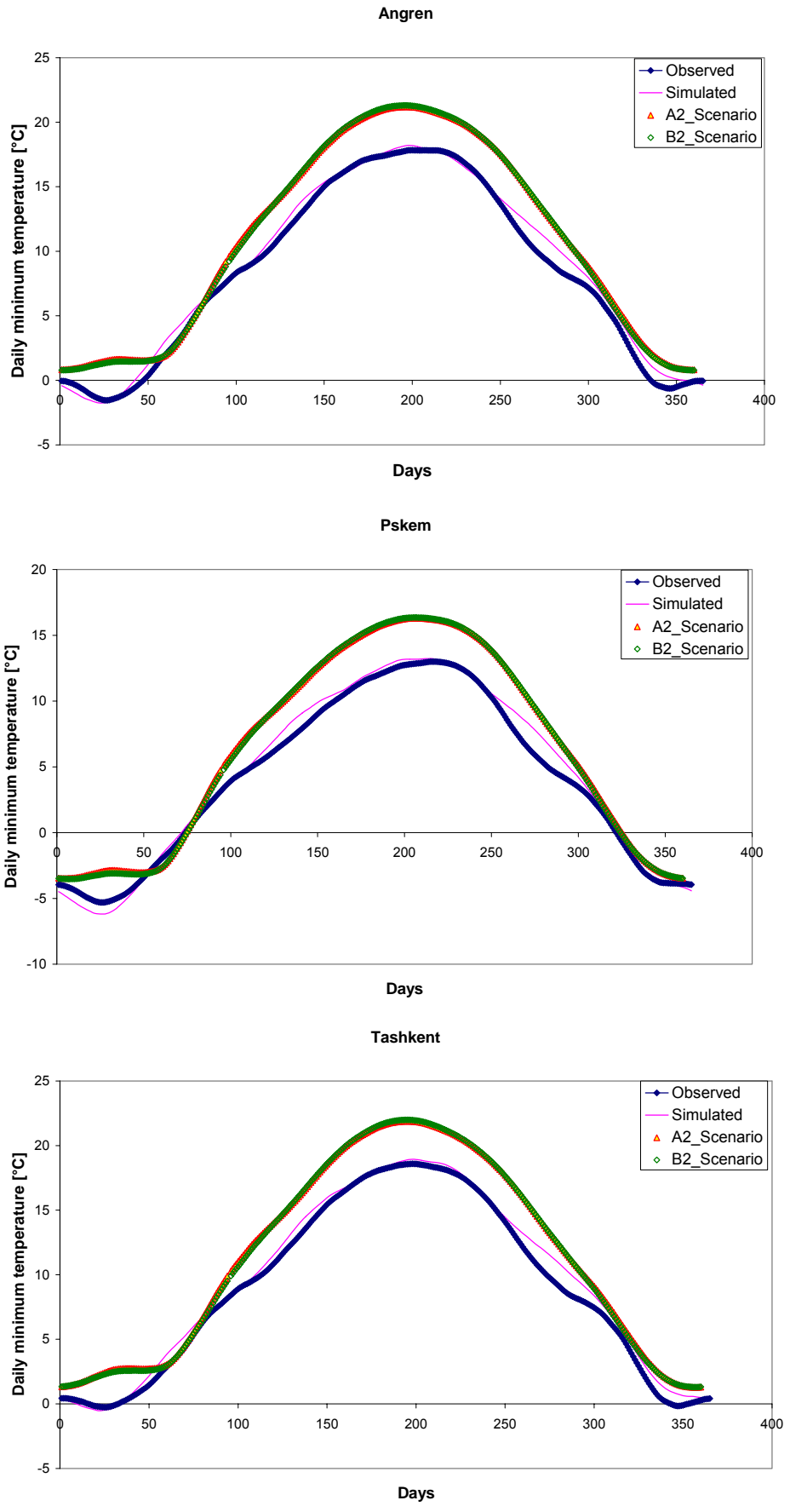


**Figure 20: Downscaled daily minimum temperature derived from A2 and B2 scenarios**

## 5 Conclusion

The downscaling models for the Chirchik – Ahangaran river basin are set up successfully and are able to capture the main variability of meteorological parameters of interest. There is a good consistency between observed and simulated daily precipitation and temperature that is proved by the annual cycle at selected stations and diagnostic indices related to extreme events, though the data source is quite limited. On the whole, our models are applicable under a subtropical climate condition and with limited data resources.

In addition, analysis of the dependence between the precipitation series and the moisture flux highlighted the influence of large-scale meteorological motion. The westward moisture flux is proved to be a dominant factor for the Chirchik - Ahangran regions.

The calibrated models are further applied to downscale meteorological variables for scenarios provided by GCMs to study the impact of climate change on the local climate condition, for instance, how much water is available and how warm and cold the future can be.

Conditioned to A2 and B2 ensembles generated by ECHAM4, it is found that there is likely to be less precipitation in spring and summer. That is, the available water resource will be reduced as a result of a lower input. In contrast, due to an increase of temperature in the future, there maybe more water from snow-melt available at the beginning of the year. Unfortunately, the summer will be even dryer and warmer than present. The maximum temperature will increase by more than 4 °C and the minimum temperature by more than 3 °C.

Appendix I:

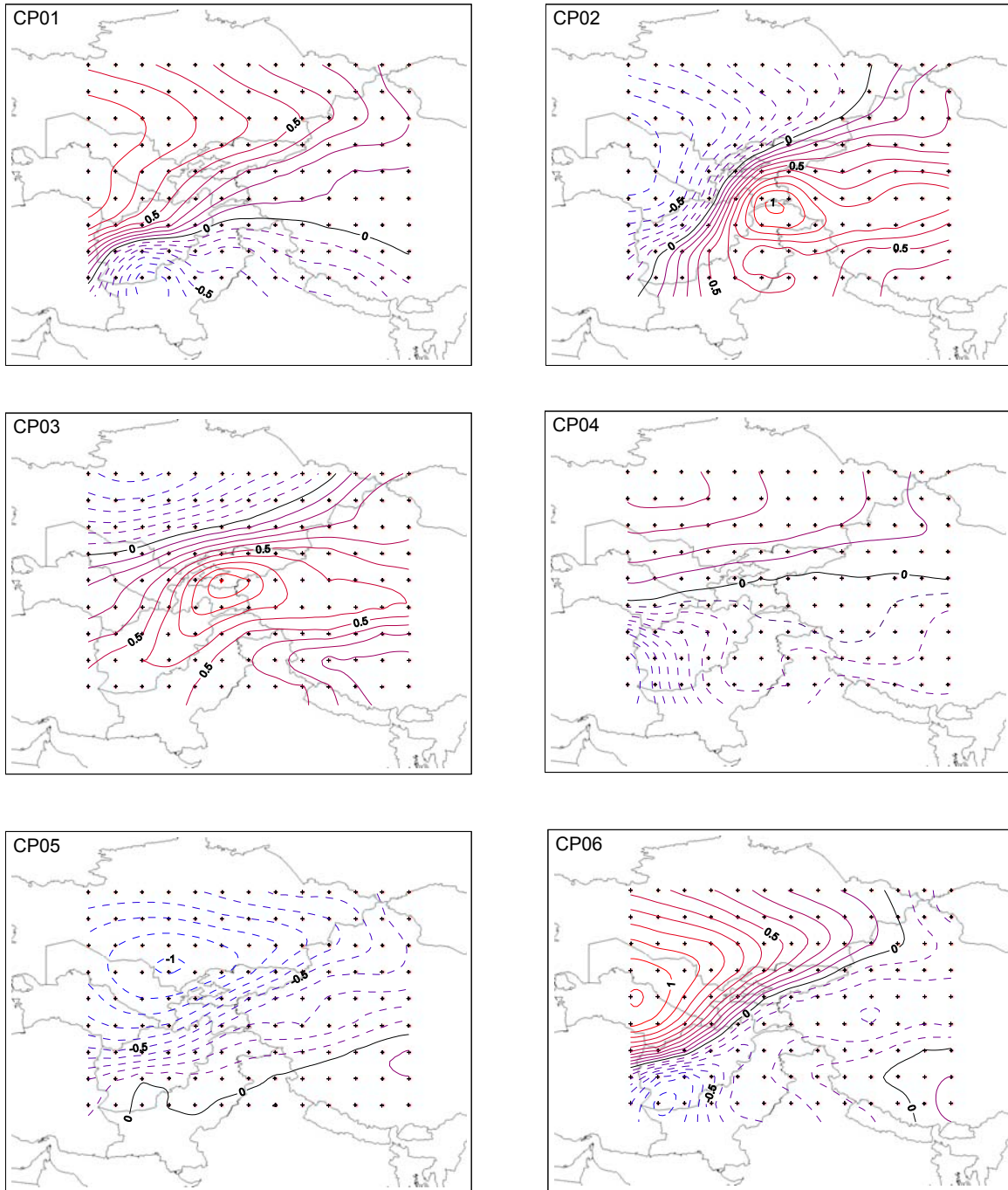
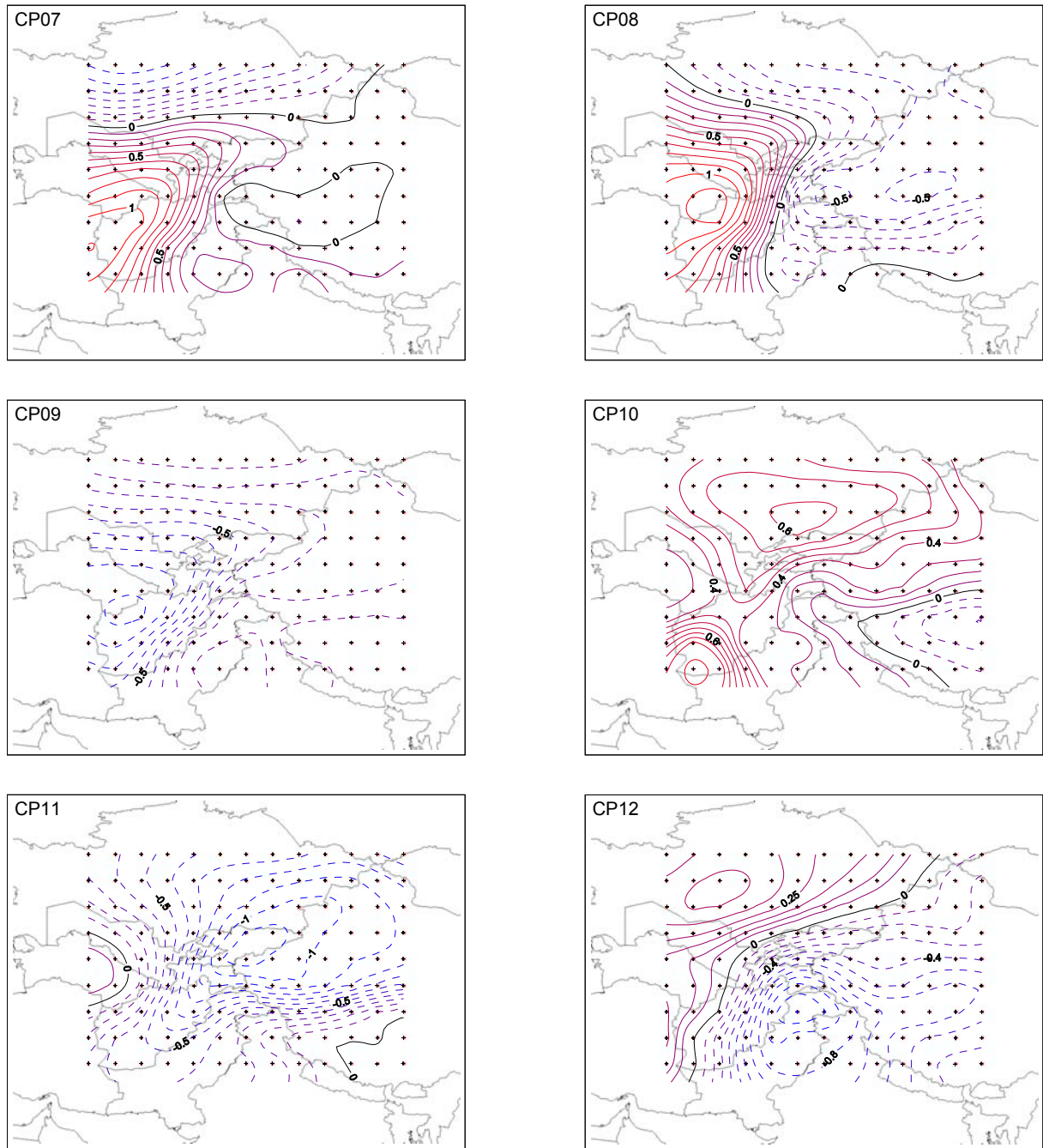


Figure 21: Anomaly maps of circulation patterns generated for precipitation: CP01-CP06 [Continued]



**Figure 22:** Anomaly maps of circulation patterns generated for precipitation: CP07-CP12 [Continued]

Appendix II:

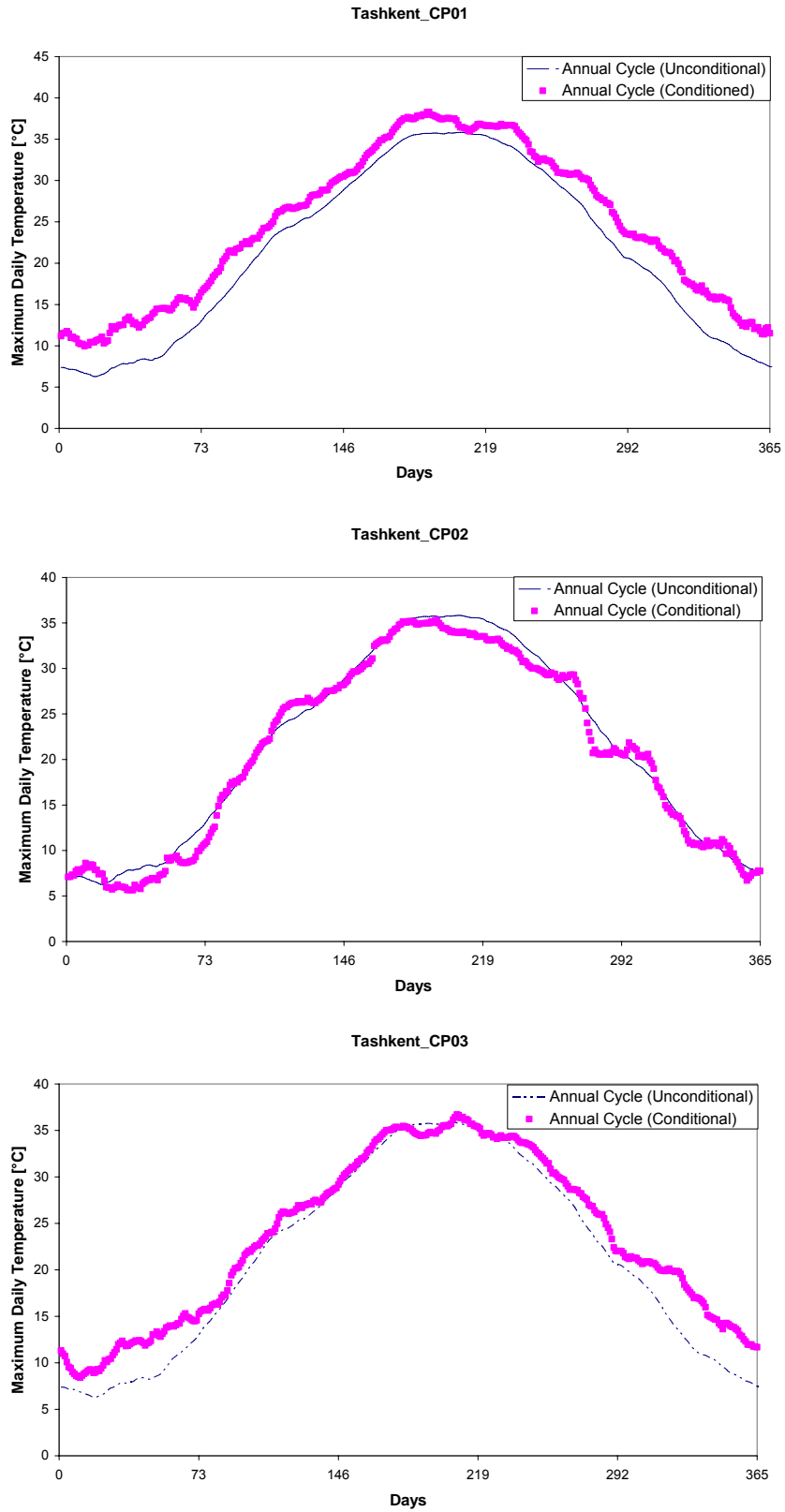
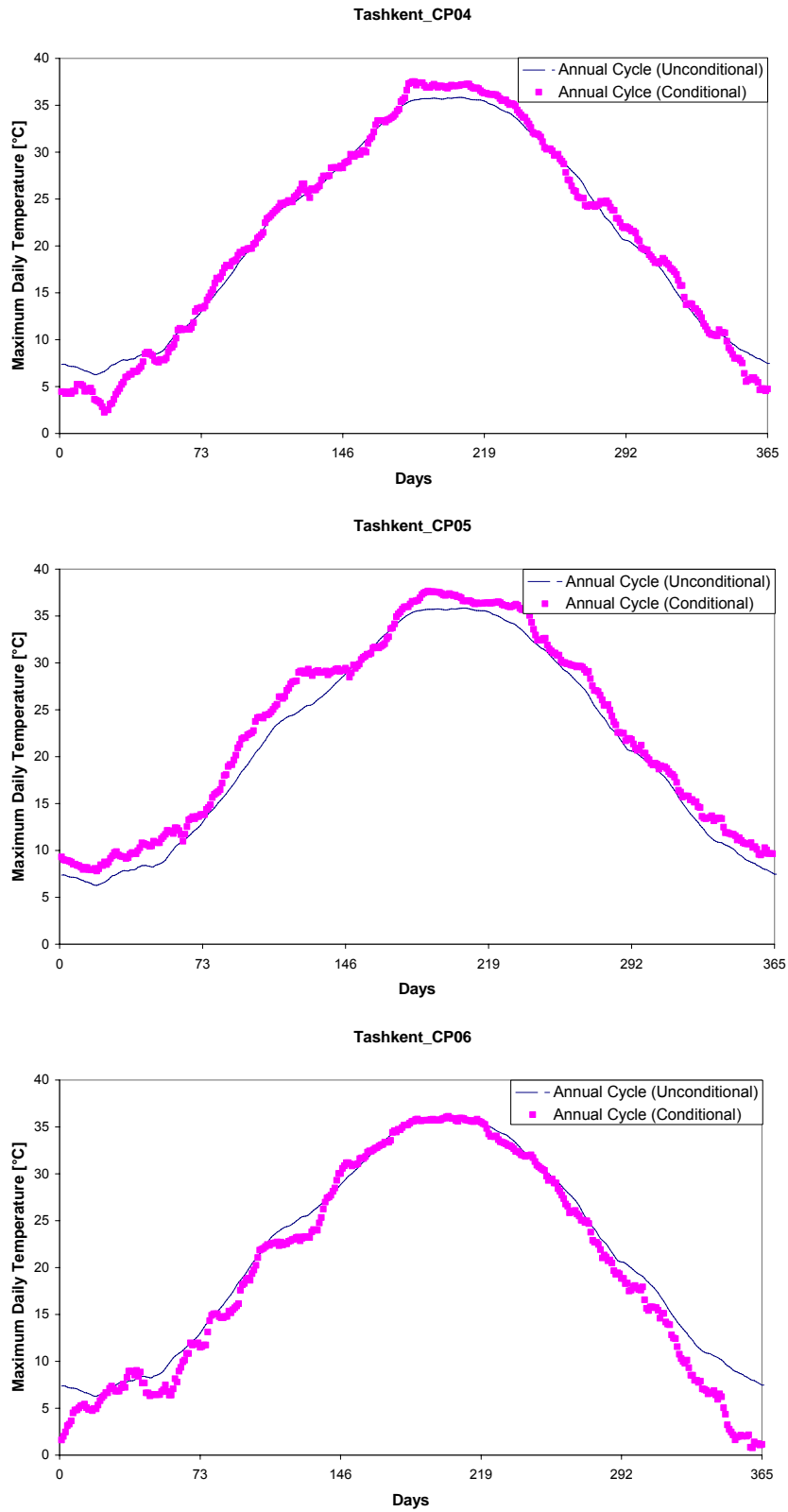
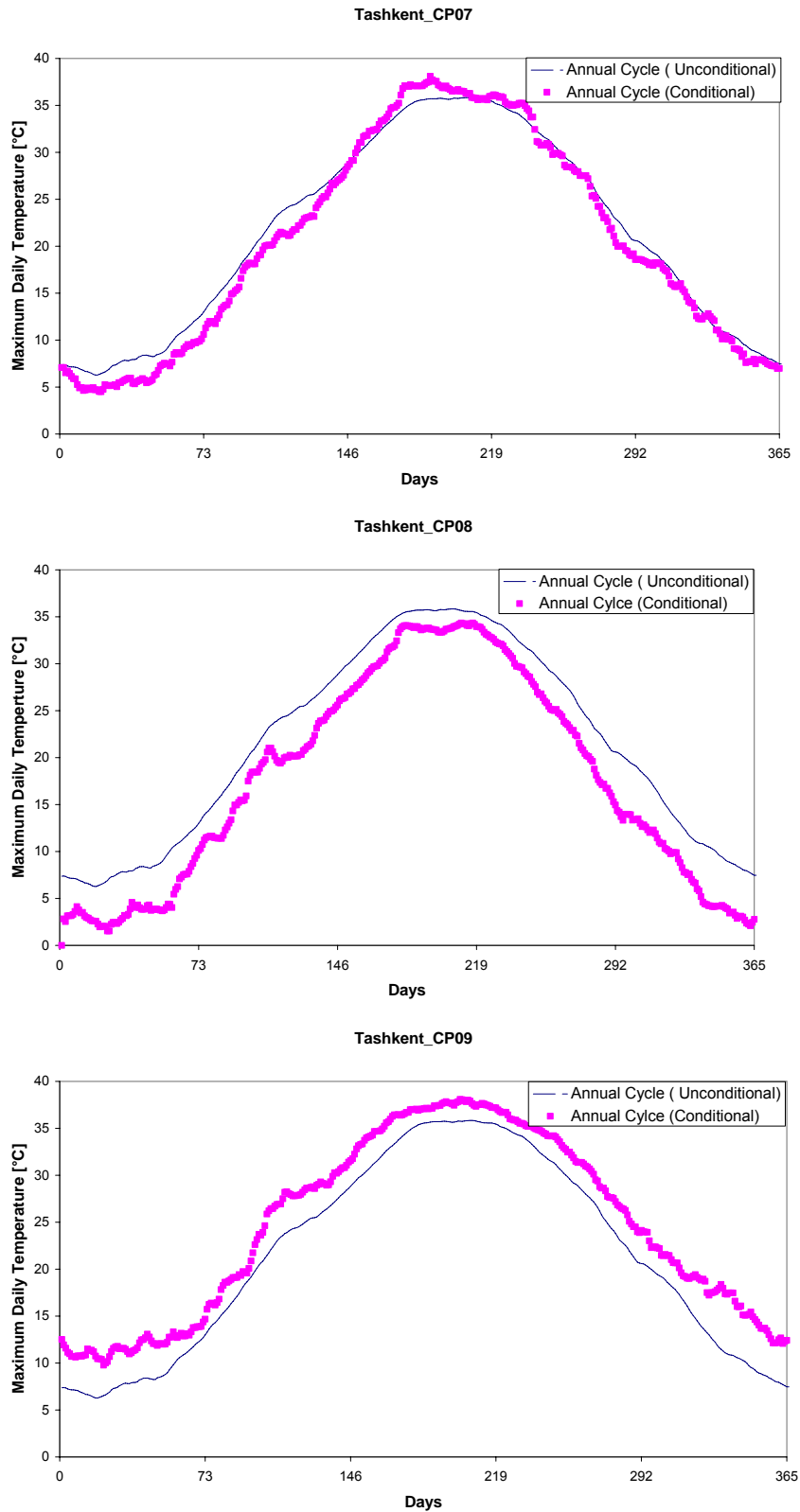


Figure 23: Average annual cycle of temperature under condition of different CPs [CP01-CP06]



**Figure 24:** Average annual cycle of temperature under condition of different CPs [CP04-CP06]



**Figure 25: Average annual cycle of temperature under condition of different CPs [CP07-CP09]**

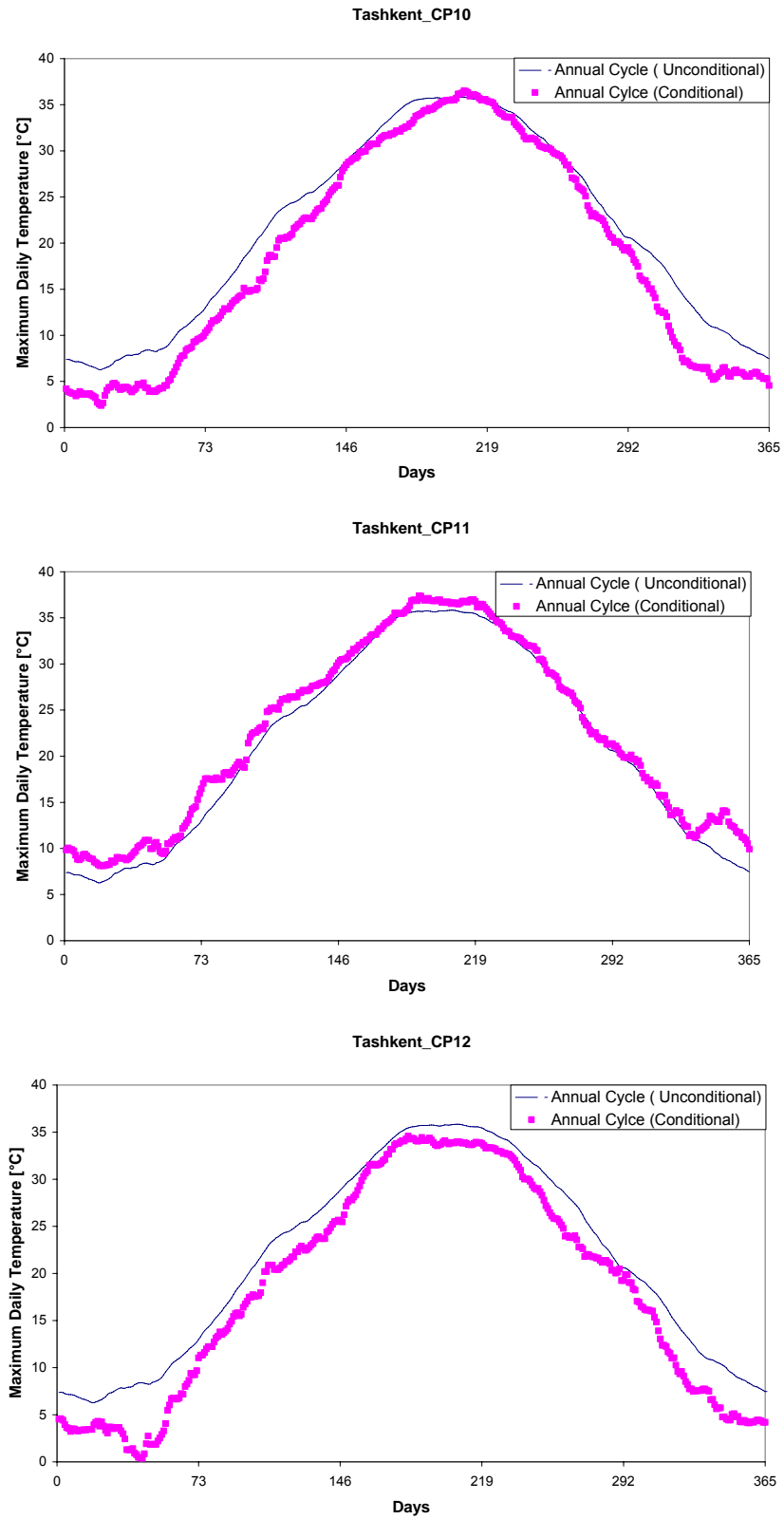


**Figure 26: Average annual cycle of temperature under condition of different CPs [CP10-CP12]**

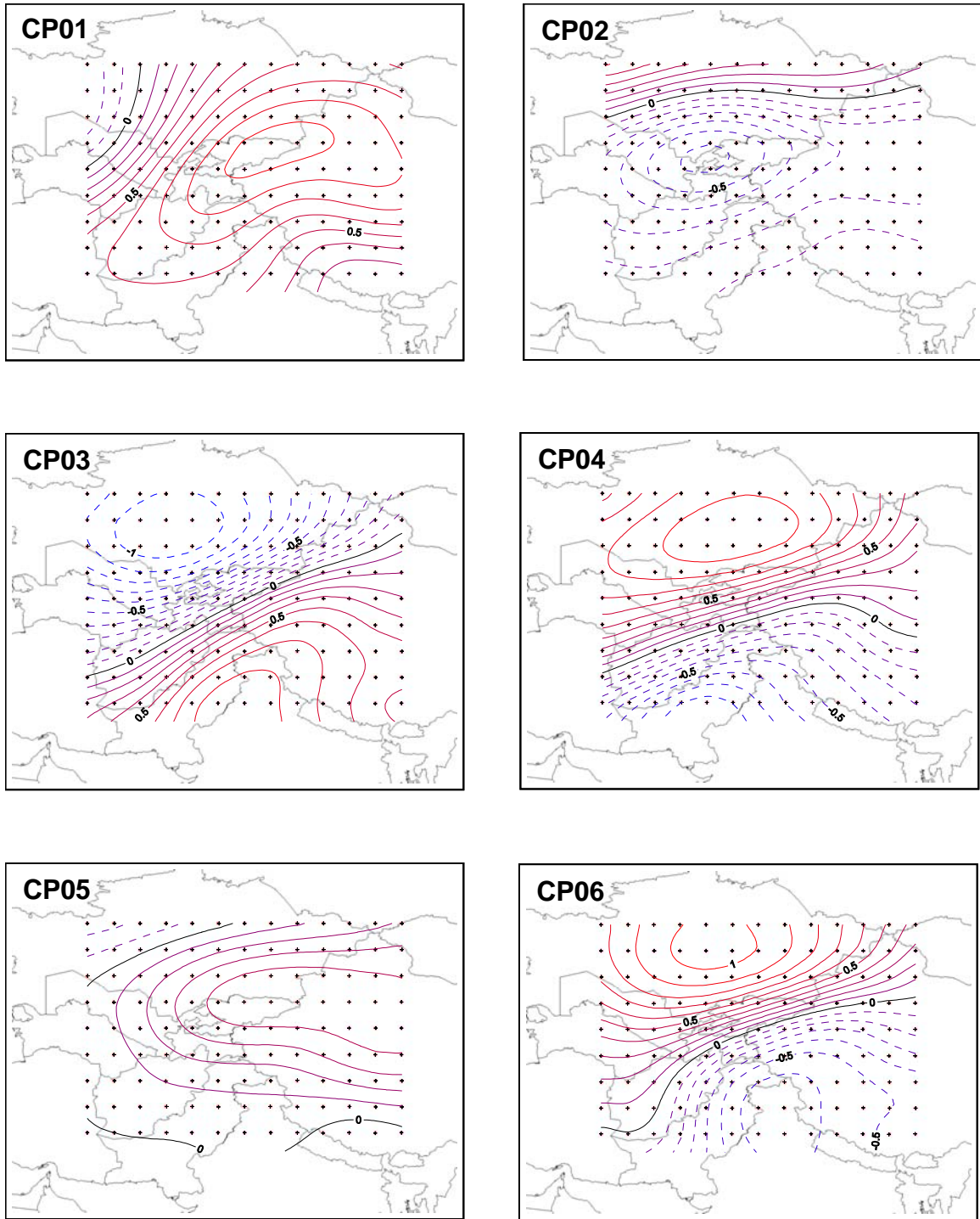


Figure 27: Anomaly maps of temperature circulation patterns of CP01-CP06 [Continued]

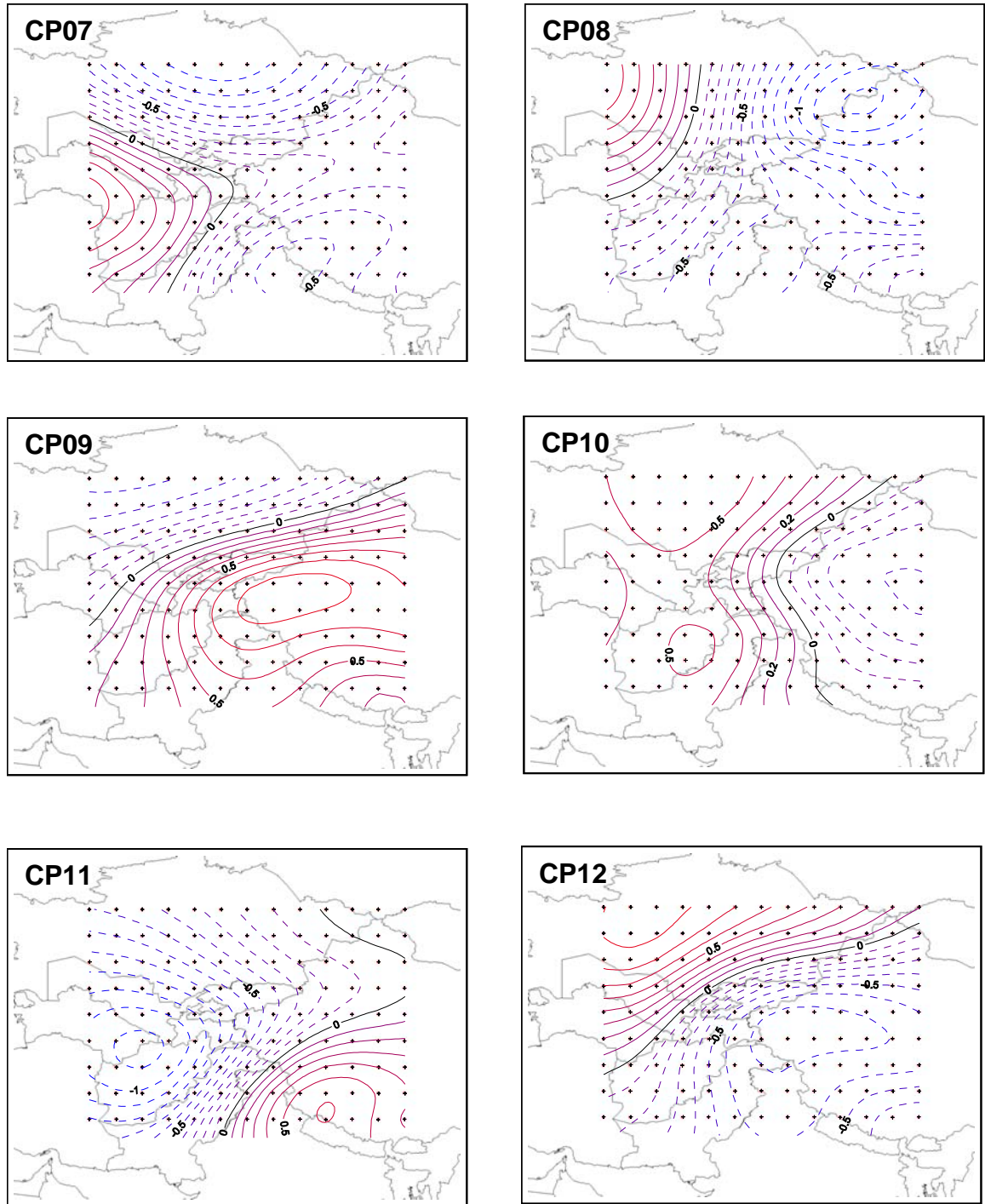


Figure 28: Anomaly maps of temperature circulation patterns of CP07-CP12 [Continued]